

$B \rightarrow X_s l^+ l^-$ in the minimal gauged $(B - L)$ supersymmetry

Tai-Fu Feng*, Jin-Lei Yang, Hai-Bin Zhang†, Shu-Min Zhao, Rong-Fei Zhu

*Department of Physics, Hebei University, Baoding, 071002, China***Abstract**

Applying the effective Hamilton for $b \rightarrow sl^+l^-$, ($l = e, \mu$) in the framework of minimal supersymmetric extension of the standard model with local $B - L$ gauge symmetry, we investigate branching ratios and forward-backward asymmetries of rare decay $B \rightarrow X_s l^+ l^-$ in low and high q^2 regions, respectively. In addition we also study the CP asymmetries depending on new CP phases from soft breaking terms in low and high q^2 regions. With some assumptions on parameter space of the model, the numerical analyses of the supersymmetric contributions to the branching ratios, forward-backward and CP asymmetries of $B \rightarrow X_s l^+ l^-$ are presented in low and high q^2 regions, respectively.

PACS numbers: 12.60.Jv, 14.60.St, 14.80.Cp

Keywords: supersymmetry, gauge symmetry, rare B decay

* email:fengtf@hbu.edu.cn

† email:hbzhang@hbu.edu.cn

I. INTRODUCTION

The study on rare B decays can detect new physics beyond the standard model (SM) since the theoretical evaluations of corresponding observations are not seriously affected by the uncertainties originating from unperturbative QCD effects. So far the Charmless semileptonic B decays are studied extensively in the SM, the authors of Ref.[1–4] analyze the QCD corrections to the branching ratios of rare B -decay, and the authors of Ref.[5–7] present corrections from $c\bar{c}$ resonances to the branching ratio of $B \rightarrow X_s l^+ l^-$. In order to obtain the QCD evolution effects precisely in rare B -decay, the relevant two-loop QCD anomalous dimension matrix (ADM) for all the flavour-changing four-quark dimension-six operators is given in Ref.[8].

Considering those corrections mentioned above, one obtains the theoretical evaluations in the SM as[9–11]

$$\begin{aligned} BR(B \rightarrow X_s l^+ l^-)_{q^2 \in [1, 6] \text{ GeV}^2}^{SM} &= (1.59 \pm 0.11) \times 10^{-6}, \\ BR(B \rightarrow X_s l^+ l^-)_{q^2 \in [14.4, 25] \text{ GeV}^2}^{SM} &= (2.3 \pm 0.7) \times 10^{-7}, (l = e, \mu). \end{aligned} \quad (1)$$

Only the contributions to the branching ratios in the low q^2 region with $1 \text{ GeV}^2 \leq q^2 \leq 6 \text{ GeV}^2$ and the high q^2 region with $14.4 \text{ GeV}^2 \leq q^2 \leq 25 \text{ GeV}^2$ are evaluated respectively. Here $q^2 = (p_{l^+} + p_{l^-})^2$ denotes the dilepton invariant mass squared. Averaging available experimental data from BaBar[12] and Belle[13], we obtain the experimental averages for the branching ratios in two regions as follows[14]

$$\begin{aligned} BR(B \rightarrow X_s l^+ l^-)_{q^2 \in [1, 6] \text{ GeV}^2}^{exp} &= (1.63 \pm 0.50) \times 10^{-6}, \\ BR(B \rightarrow X_s l^+ l^-)_{q^2 \in [14.4, 25] \text{ GeV}^2}^{exp} &= (4.3 \pm 1.2) \times 10^{-7}, (l = e, \mu). \end{aligned} \quad (2)$$

Obviously the SM theoretical evaluations on those branching ratios coincide with the experimental data in three standard deviations, and the coming precise measurements on the rare B -decay processes will set more strong constraints on the new physics beyond SM. The main purpose of investigation of B -decays is to search for traces of new physics and determine its parameter space. Besides the branching ratios, the forward-backward asymmetries in the process $B \rightarrow X_s l^+ l^-$ ($l = e, \mu$) are the physics quantities to detect new physics beyond the

SM. The updated experimental data from Belle Collaboration[15] are

$$\begin{aligned} A_{FB}(B \rightarrow X_s l^+ l^-) \Big|_{q^2 \in [1, 6] \text{ GeV}^2}^{exp} &= 0.30 \pm 0.24 \pm 0.03 , \\ A_{FB}(B \rightarrow X_s l^+ l^-) \Big|_{q^2 \in [14.4, 25] \text{ GeV}^2}^{exp} &= 0.28 \pm 0.15 \pm 0.01 , \end{aligned} \quad (3)$$

where the first uncertainty is statistical and the second uncertainty is systematic. The corresponding SM predictions are given in Ref.[16] as:

$$\begin{aligned} A_{FB}(B \rightarrow X_s l^+ l^-) \Big|_{q^2 \in [1, 6] \text{ GeV}^2}^{SM} &= -0.07 \pm 0.04 , \\ A_{FB}(B \rightarrow X_s l^+ l^-) \Big|_{q^2 \in [14.4, 25] \text{ GeV}^2}^{SM} &= 0.40 \pm 0.04 . \end{aligned} \quad (4)$$

For the present experimental uncertainty is large, we cannot yet apply the experimental data of the physics quantity to test the SM precisely. Nevertheless, the future experimental data will constrain the parameter space of new physics strongly with accumulating of data sample.

Meanwhile the SM evaluation of the CP asymmetry in the entire q^2 region is very small [17], the theoretical prediction on the CP asymmetry may be enhanced significantly [18]. The updated experimental data on the CP asymmetry from Babar Collaboration are[19]

$$\begin{aligned} A_{CP}(B \rightarrow X_s l^+ l^-) \Big|_{q^2 \in [1, 6] \text{ GeV}^2}^{exp} &= -0.06 \pm 0.22 \pm 0.01 , \\ A_{CP}(B \rightarrow X_s l^+ l^-) \Big|_{q^2 \in [14.4, 25] \text{ GeV}^2}^{exp} &= 0.19_{-0.17}^{+0.18} \pm 0.01 . \end{aligned} \quad (5)$$

In supersymmetric extensions of the SM, new sources of flavor and CP violations may appear in those soft breaking terms[20]. Actually the analyses of constraints on extensions of the SM are extensively discussed in literature. The calculation of the branching ratio of inclusive decay $B \rightarrow X_s \gamma$ is presented by authors of [21–23] in the two-Higgs doublet model (2HDM). The supersymmetric effect on $B \rightarrow X_s \gamma$ is discussed in [24–28] and the next-to-leading order (NLO) QCD corrections are given in [29]. The transition $b \rightarrow s \gamma \gamma$ in the supersymmetric extensions of the SM is computed in [30]. The hadronic B decays[31] and CP-violation in those processes[32] have been discussed also. The authors of [33] have discussed possibility to observe supersymmetric effects in rare decays $B \rightarrow X_s \gamma$ and $B \rightarrow X_s e^+ e^-$ at the B -factory. Studies on decays $B \rightarrow (K, K^*) \mu^+ \mu^-$ in the SM and supersymmetric models have been carried out in [34], a relevant review can be found in

Ref.[35] also. The theoretical analyses on oscillations of $B_0 - \bar{B}_0$ ($K_0 - \bar{K}_0$) have been done in the SM and 2HDM. In supersymmetric extensions of the SM, the calculation involving the gluino contributions should be re-studied carefully for gluino has a nonzero mass. At the NLO approximation, the QCD corrections to the $B_0 - \bar{B}_0$ mixing in the supersymmetry extensions have been discussed also. Adopting the mass-insertion approximation (MIA) method the authors of [36–38] estimate QCD corrections to the $B_0 - \bar{B}_0$ mixing, and later we have re-derived the formulation by including the contribution of gluinos [39].

The discovery of Higgs on the Large Hadron Collider (LHC) implies that the searching of particle spectrum predicted by the SM is finished now [40, 41]. One main target of particle physics is testing the SM precisely and searching for the new physics (NP) beyond it. The updated bound from ATLAS collaboration on the gluino mass is $m_{\tilde{g}} \geq 1460$ GeV, and the bound on the mass of scalar top is $m_{\tilde{t}} \geq 780$ GeV[42]. Additionally the LHCb experiment can measure the quantities of exclusive hadronic, semi-leptonic, and leptonic B and B_s decays at a high sensitivity[43]. The measurements on inclusive rare B decay and decays with neutrino final states will be performed also in two next generation B factories in near future [44, 45].

The discrete symmetry R-parity in supersymmetry is defined through $R = (-1)^{3(B-L)+2S}$, where B , L and S are baryon number, lepton number and spin respectively for a concerned field[46]. In the minimal supersymmetric extension of SM (MSSM) with local $U(1)_{B-L}$ symmetry, R-parity is spontaneously broken when left- and right-handed sneutrinos acquire nonzero vacuum expectation values (VEVs)[47–50]. Meanwhile, the nonzero VEVs of left- and right-handed sneutrinos induce the mixing between neutralinos (charginos) and neutrinos (charged leptons). Furthermore, the MSSM with local $U(1)_{B-L}$ symmetry naturally predicates two sterile neutrinos [51–53], which are favored by the Big-bang nucleosynthesis (BBN) in cosmology[54]. In other words, there are exotic sources to mediate flavor changing neutral current processes (FCNC) in this model.

Here we investigate some interesting physical quantities in the FCNC processes $B \rightarrow X_s l^+ l^-$, ($l = e, \mu$) in the MSSM with local $U(1)_{B-L}$ symmetry, our presentation is organized as follows. In section II, we briefly summarize the main ingredients of the MSSM with local $U(1)_{B-L}$ symmetry, then present effective Hamilton for $b \rightarrow s l^+ l^-$ in section III. The

formulae of decay widths, forward-backward asymmetries, CP asymmetries at hadronic scale are given in IV, respectively. The numerical analyses are given in section V, and our conclusions are summarized in section VI finally.

II. THE MSSM WITH LOCAL $U(1)_{B-L}$ SYMMETRY

When $U(1)_{B-L}$ is a local gauge symmetry, one can enlarge the local gauge group of the SM to $SU(3)_C \otimes SU(2)_L \otimes U(1)_Y \otimes U(1)_{(B-L)}$. In the model proposed in Ref.[47–50], the exotic superfields are three generation right-handed neutrinos $\hat{N}_i^c \sim (1, 1, 0, 1)$. Meanwhile, quantum numbers of the matter chiral superfields for quarks and leptons are given by

$$\begin{aligned} \hat{Q}_I &= \begin{pmatrix} \hat{U}_I \\ \hat{D}_I \end{pmatrix} \sim (3, 2, \frac{1}{3}, \frac{1}{3}), \quad \hat{L}_I = \begin{pmatrix} \hat{\nu}_I \\ \hat{E}_I \end{pmatrix} \sim (1, 2, -1, -1), \\ \hat{U}_I^c &\sim (3, 1, -\frac{4}{3}, -\frac{1}{3}), \quad \hat{D}_I^c \sim (3, 1, \frac{2}{3}, -\frac{1}{3}), \quad \hat{E}_I^c \sim (1, 1, 2, 1), \end{aligned} \quad (6)$$

with $I = 1, 2, 3$ denoting the index of generation. In addition, the quantum numbers of two Higgs doublets are assigned as

$$\hat{H}_u = \begin{pmatrix} \hat{H}_u^+ \\ \hat{H}_u^0 \end{pmatrix} \sim (1, 2, 1, 0), \quad \hat{H}_d = \begin{pmatrix} \hat{H}_d^0 \\ \hat{H}_d^- \end{pmatrix} \sim (1, 2, -1, 0). \quad (7)$$

The superpotential of the MSSM with local $U(1)_{B-L}$ symmetry is written as

$$\mathcal{W} = \mathcal{W}_{MSSM} + \mathcal{W}_{(B-L)}^{(1)}. \quad (8)$$

Here \mathcal{W}_{MSSM} is superpotential of the MSSM, and

$$\mathcal{W}_{(B-L)}^{(1)} = (Y_N)_{IJ} \hat{H}_u^T i\sigma_2 \hat{L}_I \hat{N}_J^c. \quad (9)$$

Correspondingly, the soft breaking terms for the MSSM with local $U(1)_{B-L}$ symmetry are generally given as

$$\mathcal{L}_{soft} = \mathcal{L}_{soft}^{MSSM} + \mathcal{L}_{soft}^{(1)}. \quad (10)$$

Here $\mathcal{L}_{soft}^{MSSM}$ is soft breaking terms of the MSSM, and

$$\begin{aligned} \mathcal{L}_{soft}^{(1)} &= -(m_{\tilde{N}^c}^2)_{IJ} \tilde{N}_I^{c*} \tilde{N}_J^c - (m_{BL} \lambda_{BL} \lambda_{BL} + m_{1BL} \lambda_1 \lambda_{BL} + h.c.) \\ &\quad + \left\{ (A_N)_{IJ} H_u^T i\sigma_2 \tilde{L}_I \tilde{N}_J^c + h.c. \right\}, \end{aligned} \quad (11)$$

with λ_{BL} denoting the gaugino of $U(1)_{B-L}$, m_{1BL} denoting the mixing mass parameter between the $U(1)_Y$ gaugino and $U(1)_{B-L}$ gaugino, respectively. After the $SU(2)_L$ doublets H_u , H_d , \tilde{L}_I and $SU(2)_L$ singlets \tilde{N}_I^c acquire the nonzero VEVs,

$$\begin{aligned} H_u &= \begin{pmatrix} H_u^+ \\ \frac{1}{\sqrt{2}}(v_u + H_u^0 + iP_u) \end{pmatrix}, \\ H_d &= \begin{pmatrix} \frac{1}{\sqrt{2}}(v_d + H_d^0 + iP_d) \\ H_d^- \end{pmatrix}, \\ \tilde{L}_I &= \begin{pmatrix} \frac{1}{\sqrt{2}}(v_{L_I} + \tilde{\nu}_{L_I} + iP_{L_I}) \\ \tilde{L}_I^- \end{pmatrix}, \\ \tilde{N}_I^c &= \frac{1}{\sqrt{2}}(v_{N_I} + \tilde{\nu}_{R_I} + iP_{N_I}), \end{aligned} \quad (12)$$

the R-parity is broken spontaneously, and the local gauge symmetry $SU(2)_L \otimes U(1)_Y \otimes U(1)_{(B-L)}$ is broken down to the electromagnetic symmetry $U(1)_e$, and the neutral and charged gauge bosons acquire the nonzero masses as

$$\begin{aligned} m_Z^2 &= \frac{1}{4}(g_1^2 + g_2^2)v_{EW}^2, \\ m_W^2 &= \frac{1}{4}g_2^2v_{EW}^2, \\ m_{ZBL}^2 &= g_{BL}^2(v_N^2 + v_{EW}^2 - v_{SM}^2). \end{aligned} \quad (13)$$

Where $v_{SM}^2 = v_u^2 + v_d^2$, $v_{EW}^2 = v_u^2 + v_d^2 + \sum_{\alpha=1}^3 v_{L\alpha}^2$, $v_N^2 = \sum_{\alpha=1}^3 v_{N\alpha}^2$, and g_2 , g_1 , g_{BL} denote the gauge couplings of $SU(2)_L$, $U(1)_Y$ and $U(1)_{(B-L)}$, respectively.

To satisfy present electroweak precision observations we assume the mass of neutral $U(1)_{(B-L)}$ gauge boson $m_{ZBL} > 1$ TeV which implies $v_N > 1$ TeV when $g_{BL} < 1$, then we derive $\max((Y_N)_{ij}) \leq 10^{-6}$ and $\max(v_{L_I}) \leq 10^{-3}$ GeV[50] to explain experimental data on neutrino oscillation. Considering the minimization conditions at one-loop level, we formulate the 3×3 mass-squared matrix for right-handed sneutrinos as

$$m_{\tilde{N}^c}^2 \simeq \begin{pmatrix} \Lambda_{\tilde{N}_1^c}^2 - \Lambda_{BL}^2, & 0, & -\frac{v_{N_1}}{v_{N_3}}\Lambda_{\tilde{N}_1^c}^2 \\ 0, & \Lambda_{\tilde{N}_2^c}^2 - \Lambda_{BL}^2, & -\frac{v_{N_2}}{v_{N_3}}\Lambda_{\tilde{N}_2^c}^2 \\ -\frac{v_{N_1}}{v_{N_3}}\Lambda_{\tilde{N}_1^c}^2, & -\frac{v_{N_2}}{v_{N_3}}\Lambda_{\tilde{N}_2^c}^2, & \frac{v_{N_1}^2\Lambda_{\tilde{N}_1^c}^2 + v_{N_2}^2\Lambda_{\tilde{N}_2^c}^2}{v_{N_3}^2} - \Lambda_{BL}^2 \end{pmatrix} \quad (14)$$

with $\Lambda_{BL}^2 = m_{ZBL}^2/2 + \Delta T_{\tilde{N}}$. Where $\Delta T_{\tilde{N}}$ denotes one-loop radiative corrections to the mass matrix of right-handed sneutrinos from top, bottom, tau and their supersymmetric partners [53].

III. EFFECTIVE HAMILTON FOR $b \rightarrow sl^+l^-$, ($l = e, \mu, \tau$)

The transition $b \rightarrow sl^+l^-$ is attributed to the effective Hamilton at hadronic scale

$$\mathcal{H}_{eff} = -\frac{4G_F}{\sqrt{2}}V_{tb}V_{ts}^*[C_1\mathcal{O}_1 + C_2\mathcal{O}_2 + \sum_{i=3}^6 C_i\mathcal{O}_i + \sum_{i=7}^{10} C_i\mathcal{O}_i + \sum_{i=S,P} C_i\mathcal{O}_i], \quad (15)$$

where \mathcal{O}_i ($i = 1, 2, \dots, 10, S, P$) are defined as [55]

$$\begin{aligned} \mathcal{O}_1^u &= (\bar{s}_L\gamma_\mu T^a u_L)(\bar{u}_L\gamma^\mu T^a b_L), \quad \mathcal{O}_2^u = (\bar{s}_L\gamma_\mu u_L)(\bar{u}_L\gamma^\mu b_L), \\ \mathcal{O}_3 &= (\bar{s}_L\gamma_\mu b_L)\sum_q(\bar{q}\gamma^\mu q), \quad \mathcal{O}_4 = (\bar{s}_L\gamma_\mu T^a b_L)\sum_q(\bar{q}\gamma^\mu T^a q), \\ \mathcal{O}_5 &= (\bar{s}_L\gamma_\mu\gamma_\nu\gamma_\rho b_L)\sum_q(\bar{q}\gamma^\mu\gamma^\nu\gamma^\rho q), \quad \mathcal{O}_6 = (\bar{s}_L\gamma_\mu\gamma_\nu\gamma_\rho T^a b_L)\sum_q(\bar{q}\gamma^\mu\gamma^\nu\gamma^\rho T^a q), \\ \mathcal{O}_7 &= \frac{e}{g_s^2}m_b(\bar{s}_L\sigma_{\mu\nu}b_R)F^{\mu\nu}, \quad \mathcal{O}_8 = \frac{1}{g_s}m_b(\bar{s}_L\sigma_{\mu\nu}T^a b_R)G^{a,\mu\nu}, \\ \mathcal{O}_9 &= \frac{e^2}{g_s^2}(\bar{s}_L\gamma_\mu b_L)\bar{l}\gamma^\mu l, \quad \mathcal{O}_{10} = \frac{e^2}{g_s^2}(\bar{s}_L\gamma_\mu b_L)\bar{l}\gamma^\mu\gamma_5 l, \\ \mathcal{O}_S &= \frac{e^2}{16\pi^2}m_b(\bar{s}_L b_R)\bar{l}l, \quad \mathcal{O}_P = \frac{e^2}{16\pi^2}m_b(\bar{s}_L b_R)\bar{l}\gamma_5 l. \end{aligned} \quad (16)$$

Here we adopt the MIA to get the corrections to relevant Wilson coefficients from supersymmetric particles because the updated experiment data push the energy scale of supersymmetry far above the electroweak energy scale. Furthermore we can formulate the relevant Wilson coefficients depending on the flavor changing sources from scalar quark sectors transparently by the MIA method. At the electroweak energy scale μ_{EW} , the Wilson coefficients $C_{7,NP}(\mu_{EW})$, $C_{8,NP}(\mu_{EW})$ from the new physics beyond SM can be found in our previous work [56], other relevant Wilson coefficients are split as following

$$\begin{aligned} C_{9,NP}(\mu_{EW}) &= C_{9,NP}^\gamma(\mu_{EW}) + C_{9,NP}^Z(\mu_{EW}) + C_{9,NP}^{ZBL}(\mu_{EW}) + C_{9,NP}^{box}(\mu_{EW}), \\ C_{10,NP}(\mu_{EW}) &= C_{10,NP}^\gamma(\mu_{EW}) + C_{10,NP}^Z(\mu_{EW}) + C_{10,NP}^{ZBL}(\mu_{EW}) + C_{10,NP}^{box}(\mu_{EW}), \\ C_{S,NP}(\mu_{EW}) &= \sum_{i=1}^2 C_{S,NP}^{H_i^0}(\mu_{EW}) + C_{S,NP}^{box}(\mu_{EW}), \end{aligned}$$

$$C_{P,NP}(\mu_{EW}) = C_{P,NP}^{A^0}(\mu_{EW}) + C_{P,NP}^{box}(\mu_{EW}) , \quad (17)$$

where the superscripts γ , Z , Z_{BL} , H_i^0 , A^0 , box denote that new physics corrections to relevant Wilson coefficients originate from γ -, Z -, Z_{BL} -, H_i^0 -, A^0 - penguins and box diagrams, respectively. In order to formulate the corrections transparently, we split those pieces further as

$$\begin{aligned} C_{9,NP}^\gamma(\mu_{EW}) &= C_{9,H^\pm}^\gamma(\mu_{EW}) + C_{9,\chi^\pm}^\gamma(\mu_{EW}) + C_{9,\chi^0}^\gamma(\mu_{EW}) + C_{9,\tilde{g}}^\gamma(\mu_{EW}) + C_{9,\tilde{Z}_{BL}}^\gamma(\mu_{EW}) , \\ C_{9,NP}^Z(\mu_{EW}) &= (4s_W^2 - 1)C_{10,NP}^Z(\mu_{EW}) , \\ C_{10,NP}^Z(\mu_{EW}) &= C_{10,H^\pm}^Z(\mu_{EW}) + C_{10,\chi^\pm}^Z(\mu_{EW}) + C_{10,\chi^0}^Z(\mu_{EW}) + C_{10,\tilde{g}}^Z(\mu_{EW}) + C_{10,\tilde{Z}_{BL}}^Z(\mu_{EW}) , \\ C_{9,NP}^{Z_{BL}}(\mu_{EW}) &= C_{9,H^\pm}^{Z_{BL}}(\mu_{EW}) + C_{9,\chi^\pm}^{Z_{BL}}(\mu_{EW}) + C_{9,\chi^0}^{Z_{BL}}(\mu_{EW}) + C_{9,\tilde{g}}^{Z_{BL}}(\mu_{EW}) + C_{9,\tilde{Z}_{BL}}^{Z_{BL}}(\mu_{EW}) , \\ C_{S,NP}^{H_i^0}(\mu_{EW}) &= C_{S,H^\pm}^{H_i^0}(\mu_{EW}) + C_{S,\chi^\pm}^{H_i^0}(\mu_{EW}) + C_{S,\chi^0}^{H_i^0}(\mu_{EW}) + C_{S,\tilde{g}}^{H_i^0}(\mu_{EW}) + C_{S,\tilde{Z}_{BL}}^{H_i^0}(\mu_{EW}) , \\ C_{P,NP}^{A^0}(\mu_{EW}) &= C_{P,H^\pm}^{A^0}(\mu_{EW}) + C_{P,\chi^\pm}^{A^0}(\mu_{EW}) + C_{P,\chi^0}^{A^0}(\mu_{EW}) + C_{P,\tilde{g}}^{A^0}(\mu_{EW}) + C_{P,\tilde{Z}_{BL}}^{A^0}(\mu_{EW}) , \\ C_{9,NP}^{box}(\mu_{EW}) &= C_{9,H^\pm}^{box}(\mu_{EW}) + C_{9,\chi^\pm}^{box}(\mu_{EW}) + C_{9,\chi^0}^{box}(\mu_{EW}) + C_{9,\tilde{Z}_{BL}}^{box}(\mu_{EW}) + C_{9,\chi^0\tilde{Z}_{BL}}^{box}(\mu_{EW}) , \\ C_{10,NP}^{box}(\mu_{EW}) &= C_{10,H^\pm}^{box}(\mu_{EW}) + C_{10,\chi^\pm}^{box}(\mu_{EW}) + C_{10,\chi^0}^{box}(\mu_{EW}) + C_{10,\tilde{Z}_{BL}}^{box}(\mu_{EW}) + C_{10,\chi^0\tilde{Z}_{BL}}^{box}(\mu_{EW}) , \\ C_{S,NP}^{box}(\mu_{EW}) &= C_{S,H^\pm}^{box}(\mu_{EW}) + C_{S,\chi^\pm}^{box}(\mu_{EW}) + C_{S,\chi^0}^{box}(\mu_{EW}) + C_{S,\chi^0\tilde{Z}_{BL}}^{box}(\mu_{EW}) , \\ C_{P,NP}^{box}(\mu_{EW}) &= C_{P,H^\pm}^{box}(\mu_{EW}) + C_{P,\chi^\pm}^{box}(\mu_{EW}) + C_{P,\chi^0}^{box}(\mu_{EW}) + C_{P,\chi^0\tilde{Z}_{BL}}^{box}(\mu_{EW}) , \end{aligned} \quad (18)$$

where the concrete expressions for the corrections involving $U(1)_{B-L}$ interaction are presented in Eq.(B2).

The Wilson coefficients in Eq.(17) are calculated at the matching scale μ_{EW} , then evolved down to hadronic scale $\mu \sim m_b$ by the renormalization group equations. In order to obtain hadronic matrix elements conveniently, we define effective coefficients [55]

$$\begin{aligned} C_7^{eff} &= \frac{4\pi}{\alpha_s}C_7 - \frac{1}{3}C_3 - \frac{4}{9}C_4 - \frac{20}{3}C_5 - \frac{80}{9}C_6 , \\ C_8^{eff} &= \frac{4\pi}{\alpha_s}C_8 + C_3 - \frac{1}{6}C_4 + 20C_5 - \frac{10}{3}C_6 , \\ C_9^{eff} &= C_9^{eff,SM} + \frac{4\pi}{\alpha_s}C_9^{NP} , \\ C_{10}^{eff} &= \frac{4\pi}{\alpha_s}C_{10} , \quad C_{7,8,9,10}'^{eff} = \frac{4\pi}{\alpha_s}C_{7,8,9,10}' . \end{aligned} \quad (19)$$

In the SM, the Wilson coefficient $C_7^{eff,SM}$ and $C_{10}^{eff,SM}$ are real. Nevertheless, the Wilson coefficient $C_9^{eff,SM}$ contains slightly complex CP phase originating from the continuum part

$C_7^{eff,SM}$	$C_8^{eff,SM}$	$C_9^{eff,SM}$	$C_{10}^{eff,SM}$
-0.304	-0.167	4.211	-4.103

TABLE I: At hadronic scale $\mu = m_b \simeq 4.8\text{GeV}$, SM Wilson coefficients to NNLL accuracy.

of $u\bar{u}$ and $c\bar{c}$ loop which is proportional to $V_{ub}V_{us}^*$:

$$C_9^{eff,SM} = \frac{4\pi}{\alpha_s} C_9^{SM} + \xi_1(q^2) + \frac{V_{ub}V_{us}^*}{V_{tb}V_{ts}^*} \xi_2(q^2) , \quad (20)$$

with

$$\begin{aligned} \xi_1(q^2) &= 0.138\omega\left(\frac{q^2}{m_b^2}\right) + g\left(\frac{m_c}{m_b}, \frac{q^2}{m_b^2}\right) \left(\frac{4}{3}C_1(\mu_b) + C_2(\mu_b) + 3C_3(\mu_b) + 3C_5(\mu_b)\right) \\ &\quad + \frac{2}{3}\left(C_3(\mu_b) + C_5(\mu_b)\right) - \frac{1}{2}g\left(\frac{m_d}{m_b}, \frac{q^2}{m_b^2}\right) \left(C_3(\mu_b) + \frac{4}{3}C_4(\mu_b)\right) \\ &\quad - \frac{1}{2}g\left(1, \frac{q^2}{m_b^2}\right) \left(4C_3(\mu_b) + \frac{4}{3}C_4(\mu_b) + 3C_5(\mu_b)\right) , \\ \xi_2(q^2) &= \left[g\left(\frac{m_c}{m_b}, \frac{q^2}{m_b^2}\right) - g\left(\frac{m_u}{m_b}, \frac{q^2}{m_b^2}\right)\right] \left(\frac{4}{3}C_1(\mu_b) + C_2(\mu_b)\right) . \end{aligned} \quad (21)$$

Where the concrete expressions for $\omega(z)$, $g(x, y)$ are written respectively as [55]:

$$\begin{aligned} \omega(z) &= -\frac{2}{9}\pi^2 - \frac{4}{3}Li_2(z) - \frac{2}{3}\ln z \ln(1-z) - \frac{5+4z}{3(1+2z)}\ln(1-z) \\ &\quad - \frac{2z(1+z)(1-2z)}{3(1-z)^2(1+2z)}\ln z + \frac{5+9z-6z^2}{6(1-z)(1+2z)} , \\ g(x, y) &= \frac{8}{27} - \frac{8}{9}\ln\frac{m_b}{\mu_b} - \frac{8}{9}\ln x + \frac{16x^2}{9y} \\ &\quad - \frac{4}{9}\left(1 + \frac{2x^2}{y}\right)\sqrt{1 - \frac{4x^2}{y}} \begin{cases} \ln\left|\frac{\sqrt{y-4x^2}+\sqrt{y}}{\sqrt{y-4x^2}-\sqrt{y}}\right| - i\pi, & \text{if } y > 4x^2 \\ 2\arctan\frac{\sqrt{y}}{\sqrt{4x^2-y}}, & \text{if } y < 4x^2 \end{cases} \end{aligned} \quad (22)$$

In the limit of $x = 0$, $g(0, y) = \frac{8}{27} - \frac{8}{9}\ln\frac{m_b}{\mu_b} - \frac{8}{9}\ln y + i\frac{4}{9}\pi$. In the following numerical analysis, we take $\mu_b = m_b$ for simplification.

In our numerical analyses, we evaluate the Wilson coefficients from the SM to next-to-next-to-logarithmic (NNLL) accuracy in Table.I at hadronic energy scale. On the other hand, the corrections to the Wilson coefficients from new physics are only included to one-loop accuracy:

$$\vec{C}_{NP}(\mu) = \hat{U}(\mu, \mu_0) \vec{C}_{NP}(\mu_0) ,$$

$$\vec{C}_{NP}^{\vec{\eta}}(\mu) = \widehat{U}(\mu, \mu_0) \vec{C}_{NP}^{\vec{\eta}}(\mu_0) \quad (23)$$

with

$$\begin{aligned} \vec{C}_{NP}^T &= (C_{1,NP}, \dots, C_{6,NP}, C_{7,NP}^{eff}, C_{8,NP}^{eff}, C_{9,NP}^{eff} - Y(q^2), C_{10,NP}^{eff}), \\ \vec{C}_{NP}^{\prime, T} &= (C_{7,NP}^{\prime, eff}, C_{8,NP}^{\prime, eff}, C_{9,NP}^{\prime, eff}, C_{10,NP}^{\prime, eff}). \end{aligned} \quad (24)$$

Correspondingly the evolving matrices are approached as

$$\begin{aligned} \widehat{U}(\mu, \mu_0) &\simeq 1 - \left[\frac{1}{2\beta_0} \ln \frac{\alpha_s(\mu)}{\alpha_s(\mu_0)} \right] \widehat{\gamma}^{(0)T}, \\ \widehat{U}'(\mu, \mu_0) &\simeq 1 - \left[\frac{1}{2\beta_0} \ln \frac{\alpha_s(\mu)}{\alpha_s(\mu_0)} \right] \widehat{\gamma}'^{(0)T}, \end{aligned} \quad (25)$$

where the anomalous dimension matrices can be read from Ref. [57] as

$$\begin{aligned} \widehat{\gamma}^{(0)} &= \begin{pmatrix} -4 & \frac{8}{3} & 0 & -\frac{2}{9} & 0 & 0 & -\frac{208}{243} & \frac{173}{162} & -\frac{2272}{729} & 0 \\ 12 & 0 & 0 & \frac{4}{3} & 0 & 0 & \frac{416}{81} & \frac{70}{27} & \frac{1952}{243} & 0 \\ 0 & 0 & 0 & -\frac{52}{3} & 0 & 2 & -\frac{176}{81} & \frac{14}{27} & -\frac{6752}{243} & 0 \\ 0 & 0 & -\frac{40}{9} & -\frac{100}{9} & \frac{4}{9} & \frac{5}{6} & -\frac{152}{243} & -\frac{587}{162} & -\frac{2192}{729} & 0 \\ 0 & 0 & 0 & -\frac{256}{3} & 0 & 20 & -\frac{6272}{81} & \frac{6596}{27} & -\frac{84032}{243} & 0 \\ 0 & 0 & -\frac{256}{9} & \frac{56}{9} & \frac{40}{9} & -\frac{2}{3} & \frac{4624}{243} & \frac{4772}{81} & -\frac{37856}{729} & 0 \\ 0 & 0 & 0 & 0 & 0 & 0 & \frac{32}{3} & 0 & 0 & 0 \\ 0 & 0 & 0 & 0 & 0 & 0 & -\frac{32}{9} & \frac{28}{3} & 0 & 0 \\ 0 & 0 & 0 & 0 & 0 & 0 & 0 & 0 & 0 & 0 \\ 0 & 0 & 0 & 0 & 0 & 0 & 0 & 0 & 0 & 0 \end{pmatrix}, \\ \widehat{\gamma}'^{(0)} &= \begin{pmatrix} \frac{32}{3} & 0 & 0 & 0 \\ -\frac{32}{9} & \frac{28}{3} & 0 & 0 \\ 0 & 0 & 0 & 0 \\ 0 & 0 & 0 & 0 \end{pmatrix}. \end{aligned} \quad (26)$$

In addition, the operators $\mathcal{O}_{S,P}^{(\prime)}$ do not mix with other operators and their Wilson coefficients are given by the corresponding coefficients at matching scale.

IV. DIFFERENTIAL DECAY BRANCHING RATIOS, FORWARD-BACKWARD AND CP ASYMMETRIES

Keeping full dependence on the lepton mass while neglecting the strange quark mass, we write the unnormalized double differential decay width for $B \rightarrow X_s l^+ l^-$ ($l = e, \mu, \tau$) as

$$\begin{aligned}
\frac{d^2\Gamma}{dq^2 d\cos\theta} = & \frac{\alpha_{EW}^2}{16\pi^2} \frac{G_F^2 m_b^5 |V_{tb} V_{ts}^*|^2}{48\pi^3} \left(1 - \frac{q^2}{m_b^2}\right)^2 \sqrt{1 - \frac{4m_l^2 m_b^2}{(q^2)^2}} \\
& \times \left\{ 6 \left(1 + \frac{2m_l^2}{q^2}\right) \Re(C_7^{eff} C_9^{eff*}(q^2)) + \frac{3m_l^2}{m_b^2} [|C_9^{eff}(q^2)|^2 - |C_{10}^{eff}|^2] \right. \\
& + 3 \left(1 + \frac{2m_l^2}{q^2}\right) |C_7^{eff}|^2 \left[\frac{m_b^2}{q^2} (1 + \cos^2\theta) + (1 - \cos^2\theta) \right] \\
& + \frac{3}{4} [|C_9^{eff}(q^2)|^2 + |C_{10}^{eff}|^2] \left[(1 - \cos^2\theta) + \left(\frac{q^2 - m_l^2}{m_b^2} + \frac{m_l^2}{q^2}\right) (1 + \cos^2\theta) \right] \\
& + \frac{9}{32} q^2 \left(1 - \frac{4m_l^2}{q^2}\right) (|C_s|^2 + |C_P|^2) (1 + \cos^2\theta) \\
& + \frac{9}{4} m_l \Re(C_s C_{10}^{eff*} + C_P C_{10}^{eff*}) (1 - \cos^2\theta) \\
& - \frac{3q^2}{m_b^2} \Re(C_9^{eff}(q^2) C_{10}^{eff*}) \cos\theta - 6 \Re(C_7^{eff} C_{10}^{eff*}) \cos\theta \\
& \left. + \frac{3m_l}{2} \Re((2C_7^{eff} + C_9^{eff}(q^2))(C_s^* + C_P^*)) \cos\theta \right\}, \tag{27}
\end{aligned}$$

where θ denotes the angle between the l^+ and B meson three momenta in the di-lepton rest frame. In order to reduce the uncertainties originating from the bottom quark mass and CKM matrix elements, one generally normalize the observables by the semileptonic decay width of B meson:

$$\Gamma(B \rightarrow X_c e \bar{\nu}_e) = \frac{G_F^2 m_b^5}{192\pi^3} |V_{cb}|^2 f(z) \kappa(z). \tag{28}$$

Here $f(z) = 1 - 8z^2 + 8z^6 - z^8 - 24z^4 \ln z$ is phase space factor, $\kappa(z) = 1 - 2\alpha_s/3\pi[(\pi^2 - 31/4)(1 - z)^2 + 3/2]$ is the QCD correction factor with $z = m_c/m_b$ [58], respectively. Using Eq.(27) and Eq.(28), we get the normalized differential decay branching ratio of $B \rightarrow X_s l^+ l^-$ ($l = e, \mu, \tau$) at hadronic scale as

$$R(q^2) = \frac{1}{\Gamma(B \rightarrow X_c e \nu)} \frac{d\Gamma(B \rightarrow X_s l^+ l^-)}{dq^2}$$

$$\begin{aligned}
&= \frac{\alpha_{\text{EW}}^2}{4\pi^2} \left| \frac{V_{tb} V_{ts}^*}{V_{cb}} \right|^2 \frac{1}{f(z)k(z)} \left(1 - \frac{q^2}{m_b^2}\right)^2 \sqrt{1 - \frac{4m_l^2 m_b^2}{(q^2)^2}} \\
&\quad \times \left\{ 4 \left(1 + \frac{2m_l^2}{q^2}\right) \left[3\Re(C_7^{\text{eff}} C_9^{\text{eff}*}(q^2)) + \left(1 + \frac{2m_b^2}{q^2}\right) |C_7^{\text{eff}}|^2 \right] \right. \\
&\quad + \left(1 + \frac{2q^2}{m_b^2} + \frac{2m_l^2}{q^2} + \frac{4m_l^2}{m_b^2}\right) |C_9^{\text{eff}}(q^2)|^2 \\
&\quad + \left(1 + \frac{2q^2}{m_b^2} + \frac{2m_l^2}{q^2} - \frac{8m_l^2}{m_b^2}\right) |C_{10}^{\text{eff}}|^2 \\
&\quad + \frac{3}{4} q^2 \left(1 - \frac{4m_l^2}{q^2}\right) (|C_S|^2 + |C_P|^2) \\
&\quad \left. + 3m_l \Re(C_S C_{10}^{\text{eff}*} + C_P C_{10}^{\text{eff}*}) \right\} , \tag{29}
\end{aligned}$$

where $q^2 = (p_{l^+} + p_{l^-})^2$ denotes the dilepton invariant mass squared. Meanwhile the unnormlized forward-backward asymmetry is formulated as

$$\begin{aligned}
\bar{A}_{FB}(q^2) &= \frac{1}{\Gamma(B \rightarrow X_c e \nu)} \int_{-1}^1 d\cos\theta \frac{d^2\Gamma(B \rightarrow X_s l^+ l^-)}{d\cos\theta dq^2} \text{Sgn}(\cos\theta) \\
&= -\frac{3\alpha_{\text{EW}}^2}{4\pi^2} \left| \frac{V_{tb} V_{ts}^*}{V_{cb}} \right|^2 \frac{1}{f(z)k(z)} \left(1 - \frac{q^2}{m_b^2}\right)^2 \sqrt{1 - \frac{4m_l^2 m_b^2}{(q^2)^2}} \\
&\quad \times \left\{ \frac{q^2}{m_b^2} \Re(C_9^{\text{eff}}(q^2) C_{10}^{\text{eff}*}) + 2\Re(C_7^{\text{eff}} C_{10}^{\text{eff}*}) \right. \\
&\quad \left. - \frac{m_l}{2} \Re((2C_7^{\text{eff}} + C_9^{\text{eff}}(q^2))(C_S^* + C_P^*)) \right\} , \tag{30}
\end{aligned}$$

and the normalized forward-backward asymmetry is

$$A_{FB}(q^2) = \frac{1}{R(q^2)} \bar{A}_{FB}(q^2) , \tag{31}$$

respectively. The global forward-backward asymmetry in the region $q^2 \in [a, b]$ GeV² is defined through

$$\begin{aligned}
A_{FB} \Big|_{q^2 \in [a, b] \text{ GeV}^2} &= \frac{N(l_{\rightarrow}^+) - N(l_{\leftarrow}^+)}{N(l_{\rightarrow}^+) + N(l_{\leftarrow}^+)} \Big|_{q^2 \in [a, b] \text{ GeV}^2} \\
&= \frac{\int_a^b dq^2 \bar{A}_{FB}(q^2)}{\int_a^b dq^2 R(q^2)} . \tag{32}
\end{aligned}$$

The direct CP asymmetry in $B \rightarrow X_s l^+ l^-$ is defined by

$$\begin{aligned}
A_{CP}(q^2) &= \frac{d\Gamma(B \rightarrow X_s l^+ l^-)/dq^2 - d\Gamma(\bar{B} \rightarrow \bar{X}_s l^+ l^-)/dq^2}{d\Gamma(B \rightarrow X_s l^+ l^-)/dq^2 + d\Gamma(\bar{B} \rightarrow \bar{X}_s l^+ l^-)/dq^2} \\
&= \frac{\Delta D(q^2)}{D(q^2)} , \tag{33}
\end{aligned}$$

with

$$\begin{aligned}
\Delta D(q^2) &= 2\left(1 + \frac{2m_l^2}{q^2}\right) \left\{ \Im\left(\frac{V_{ub}V_{us}^*}{V_{tb}V_{ts}^*}\right) \left[2\left(1 + \frac{2q^2}{m_b^2}\right) \Im(\xi_1\xi_2^*) - 12C_7^{eff,SM}(\mu_b) \Im(\xi_2) \right] \right. \\
&\quad + 2\left(1 + \frac{2q^2}{m_b^2}\right) \left[\Im(\xi_1) \Im(C_9^{eff,NP}(\mu_b)) + \Im(\xi_2) \Im\left(\frac{V_{ub}V_{us}^*}{V_{tb}V_{ts}^*} C_9^{eff,NP}(\mu_b)\right) \right] \\
&\quad \left. + 12\left[\Im(\xi_1) \Im(C_7^{eff,NP}(\mu_b)) + \Im(\xi_2) \Im\left(\frac{V_{ub}V_{us}^*}{V_{tb}V_{ts}^*} C_7^{eff,NP}(\mu_b)\right) \right] \right\}, \\
D(q^2) &= \left(1 + \frac{2m_l^2}{q^2}\right) \left(1 + \frac{2q^2}{m_b^2}\right) \left\{ B_1 + 2|C_9^{eff,NP}(\mu_b)|^2 + 4\Re(\xi_1)\Re(C_9^{eff,NP}(\mu_b)) \right. \\
&\quad \left. + 4\Re(\xi_2)\Re\left(\frac{V_{ub}V_{us}^*}{V_{tb}V_{ts}^*} C_9^{eff,NP}(\mu_b)\right) \right\} \\
&\quad + 12\left(1 + \frac{2m_l^2}{q^2}\right) \left\{ B_2 + 2C_7^{eff,SM}(\mu_b)\Re(C_9^{eff,NP}(\mu_b)) \right. \\
&\quad + 2\Re(C_7^{eff,NP}(\mu_b)C_9^{eff,NP*}(\mu_b)) + 2\Re(\xi_1)\Re(C_7^{eff,NP}(\mu_b)) \\
&\quad \left. + 2\Re(\xi_2)\Re\left(\frac{V_{ub}V_{us}^*}{V_{tb}V_{ts}^*} C_7^{eff,NP}(\mu_b)\right) \right\} \\
&\quad + 8\left(1 + \frac{2m_l^2}{q^2}\right) \left(1 + \frac{2m_b^2}{q^2}\right) |C_7^{eff}|^2 \\
&\quad + 2\left(1 + \frac{2q^2}{m_b^2} + \frac{2m_l^2}{q^2} - \frac{8m_l^2}{m_b^2}\right) |C_{10}^{eff}|^2 \\
&\quad + \frac{3}{2}q^2\left(1 - \frac{4m_l^2}{q^2}\right) (|C_S|^2 + |C_P|^2) \\
&\quad + 6m_l\Re(C_S C_{10}^{eff*} + C_P C_{10}^{eff*}). \tag{34}
\end{aligned}$$

Here

$$\begin{aligned}
B_1 &= 2\left\{ |\xi_1|^2 + \left|\frac{V_{ub}V_{us}^*}{V_{tb}V_{ts}^*}\xi_2\right|^2 + 2\Re\left(\frac{V_{ub}V_{us}^*}{V_{tb}V_{ts}^*}\right)\Re(\xi_1\xi_2) \right\}, \\
B_2 &= 2C_7^{eff,SM}(\mu_b) \left\{ \Re(\xi_1) + \Re\left(\frac{V_{ub}V_{us}^*}{V_{tb}V_{ts}^*}\right)\Re(\xi_2) \right\}. \tag{35}
\end{aligned}$$

The global CP asymmetry in the region $q^2 \in [a, b]$ GeV² is correspondingly defined through

$$A_{CP} \Big|_{q^2 \in [a, b] \text{ GeV}^2} = \frac{\int_a^b dq^2 \Delta D(q^2)}{\int_a^b dq^2 D(q^2)}. \tag{36}$$

In the region $1\text{GeV}^2 \leq q^2 \leq 6\text{GeV}^2$ where the theoretical evaluations are not heavily affected by the photon pole at low q^2 and the $c\bar{c}$ resonances at higher q^2 , the updated

theoretical predictions in this region are[59]:

$$\begin{aligned} Br(B \rightarrow X_s e^+ e^-) \Big|_{q^2 \in [1, 6] \text{ GeV}^2}^{SM} &= (1.64 \pm 0.11) \times 10^{-6}, \\ Br(B \rightarrow X_s \mu^+ \mu^-) \Big|_{q^2 \in [1, 6] \text{ GeV}^2}^{SM} &= (1.59 \pm 0.11) \times 10^{-6}. \end{aligned} \quad (37)$$

In the region $q^2 \geq 14.4 \text{ GeV}^2$, the theoretical uncertainty is relatively larger than that in the low region $1 \text{ GeV}^2 \leq q^2 \leq 6 \text{ GeV}^2$, and the SM theoretical evaluations are given as[59]:

$$\begin{aligned} Br(B \rightarrow X_s e^+ e^-) \Big|_{q^2 \in [14.4, 25] \text{ GeV}^2}^{SM} &= (0.21 \pm 0.07) \times 10^{-6}, \\ Br(B \rightarrow X_s \mu^+ \mu^-) \Big|_{q^2 \in [14.4, 25] \text{ GeV}^2}^{SM} &= (0.24 \pm 0.07) \times 10^{-6}. \end{aligned} \quad (38)$$

In our analysis, the lepton-flavor-averaged branching ratio for $B \rightarrow X_s l^+ l^-$ is averages of the individual $Br(B \rightarrow X_s e^+ e^-)$ and $Br(B \rightarrow X_s \mu^+ \mu^-)$. Furthermore, the updated experimental data on the forward-backward and CP asymmetries constrain the parameter space of new physics concretely.

V. NUMERICAL ANALYSES

In order to perform our numerical analyses, we present the relevant SM inputs from [60] in table.II. The supersymmetric parameters involved here are soft breaking masses of the 2nd and 3rd generation squarks, $m_{\tilde{Q}_{2,3}}^2$, $m_{\tilde{U}_{2,3}}^2$, $m_{\tilde{D}_{2,3}}^2$, soft breaking masses of the 1st and 2nd generation sleptons $m_{\tilde{L}_{1,2}}$, $m_{\tilde{E}_{1,2}}$, $m_{\tilde{N}_{1,2}}$, neutralino and chargino masses $m_{\chi_\alpha^0}$, $m_{\chi_\beta^\pm}$, ($\alpha = 1, \dots, 4$, $\beta = 1, 2$) and their mixing matrices. Additionally the masses and mixing matrix of $B - L$ gaugino/right-handed neutrinos are mainly determined from nonzero VEVs of right-handed sneutrinos, local $B - L$ gauge coupling g_{BL} and soft gaugino mass parameters m_{BL} , m_{1BL} . The flavor conservation mixing between left- and right-handed of the third generation squarks $(\delta_u^{LR})_{33} = m_{\tilde{t}_X}^2 / \Lambda_{NP}^2$, $(\delta_d^{LR})_{33} = m_{\tilde{b}_X}^2 / \Lambda_{NP}^2$ are chosen to give the lightest Higgs mass in the range $124 - 126 \text{ GeV}$, where the concrete expressions of $m_{\tilde{t}_X}^2$, $m_{\tilde{b}_X}^2$ are presented in appendix A. The $b \rightarrow s$ transitions are mediated by those flavor changing insertions $(\delta_{U,D}^{LL})_{23}$, $(\delta_{U,D}^{LR})_{23}$, $(\delta_{U,D}^{RR})_{23}$, which are originated from flavour-violating scalar mass terms and trilinear scalar couplings in soft breaking terms.

Input	Input
$m_B = 5.280 \text{ GeV}$	$m_{K^*} = 0.896 \text{ GeV}$
$m_{B_s} = 5.367 \text{ GeV}$	$m_\mu = 0.106 \text{ GeV}$
$m_W = 80.40 \text{ GeV}$	$m_Z = 91.19 \text{ GeV}$
$\tau_B = 2.307 \times 10^{12} \text{ GeV}$	$f_B = 0.190 \pm 0.004$
$\alpha_s(m_Z) = 0.118 \pm 0.002$	$\alpha_{em}(m_Z) = 1/128.9$
$m_c(m_c) = 1.27 \pm 0.11 \text{ GeV}$	$m_b(m_b) = 4.18 \pm 0.17 \text{ GeV}$
$m_t^{pole} = 173.1 \pm 1.3 \text{ GeV}$	
$\lambda_{CKM} = 0.225 \pm 0.001$	$A_{CKM} = 0.811 \pm 0.022$
$\bar{\rho} = 0.131 \pm 0.026$	$\bar{\eta} = 0.345 \pm 0.014$

TABLE II: Input parameters[60] of the SM used in the numerical analysis

The updated bound from ATLAS collaboration on the gluino mass is $m_{\tilde{g}} \geq 1460 \text{ GeV}$, and the bound on the mass of scalar top is $m_{\tilde{t}} \geq 780 \text{ GeV}$ [42]. To coincide with those experimental data, we always assume $\Lambda_{NP} = m_{\tilde{Q}_{2,3}} = m_{\tilde{U}_{2,3}} = m_{\tilde{D}_{2,3}} = 2 \text{ TeV}$, $m_{\tilde{L}_{1,2}} = m_{\tilde{E}_{1,2}} = m_{\tilde{N}_{1,2}} = 1 \text{ TeV}$, and $m_{\tilde{g}} \geq 1.5 \text{ TeV}$ in our numerical discussion unless specified.

Certainly the experimental data of 125 GeV constrain the parameter space of supersymmetric extension of the SM strongly. The radiative corrections to mass of the lightest Higgs subtly depend on the parameters $\tan \beta$, μ , the squark masses of the third generation and relevant trilinear couplings A_t , A_b in soft terms. Furthermore the observed average on branching ratio of $B_s^0 \rightarrow \mu^+ \mu^-$ is[60]

$$BR(B \rightarrow \mu^+ \mu^-)^{exp} \simeq (3.1 \pm 0.7) \times 10^{-9}, \quad (39)$$

which coincides with the SM evaluation:

$$BR(B \rightarrow \mu^+ \mu^-)^{SM} \simeq (3.23 \pm 0.27) \times 10^{-9}. \quad (40)$$

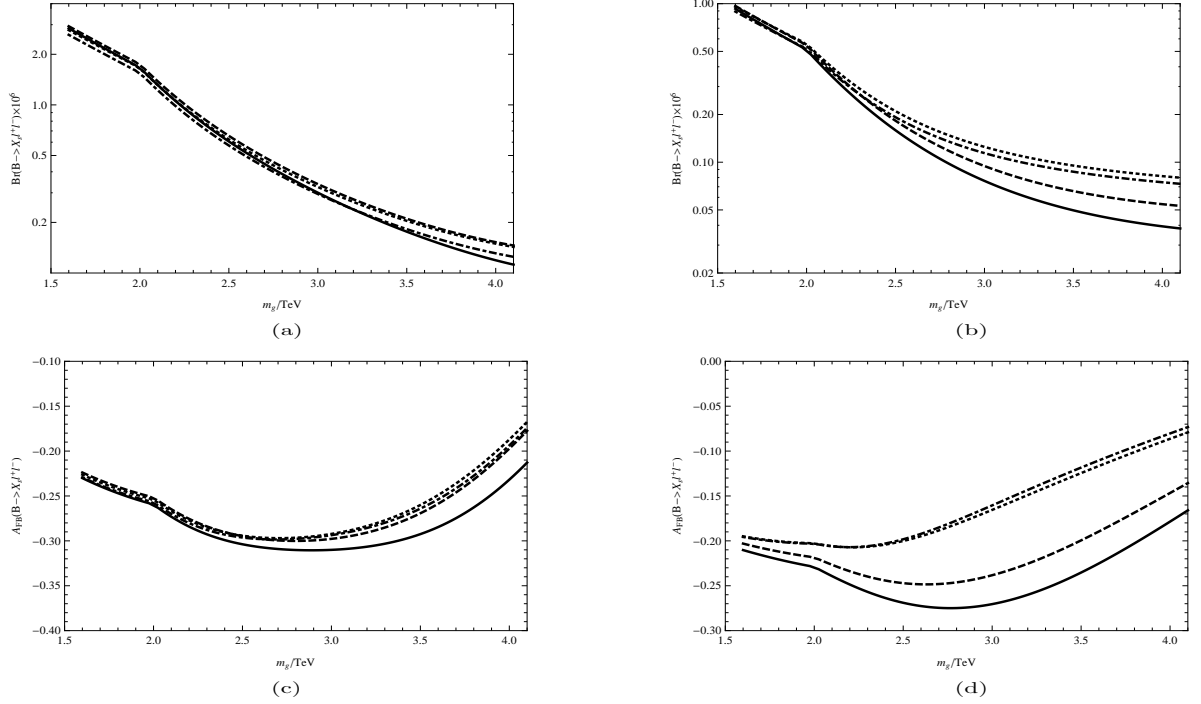


FIG. 1: Taking $(\delta_D^{LL})_{23} = (\delta_D^{RR})_{23} = (\delta_D^{LR})_{23} = 0.125$, we plot (a) $BR(B \rightarrow X_s l^+ l^-)_{q^2 \in [1, 6] \text{ GeV}^2} \times 10^6$, (b) $BR(B \rightarrow X_s l^+ l^-)_{q^2 \in [14.4, 25.0] \text{ GeV}^2} \times 10^6$ (c) $A_{FB}(B \rightarrow X_s l^+ l^-)_{q^2 \in [1, 6] \text{ GeV}^2}$, (d) $A_{FB}(B \rightarrow X_s l^+ l^-)_{q^2 \in [14.4, 25.0] \text{ GeV}^2}$, varying with the gluino mass. Where the solid lines denote $\tan \beta = 5$, dashed lines denote $\tan \beta = 10$, dotted lines denote $\tan \beta = 30$, dashed-dotted lines denote $\tan \beta = 50$, respectively.

The average experimental data on the branching ratio of the inclusive $\bar{B} \rightarrow X_s \gamma$ reads

$$BR(\bar{B} \rightarrow X_s \gamma)^{exp} \simeq (3.40 \pm 0.21) \times 10^{-4}, \quad (41)$$

and the corresponding SM prediction at NNLO order is

$$BR(\bar{B} \rightarrow X_s \gamma)^{SM} \simeq (3.36 \pm 0.23) \times 10^{-4}. \quad (42)$$

The experimental data from $\bar{B} \rightarrow X_s \gamma$ and $B_s^0 \rightarrow \mu^+ \mu^-$ also constrain on correlations between the flavor-changing parameters and energy scale of new physics strongly.

To obtain mass of the lightest Higgs in reasonable range, we further choose the mass of CP-odd Higgs $m_A = 1 \text{ TeV}$, and the following assumptions on the parameter space.

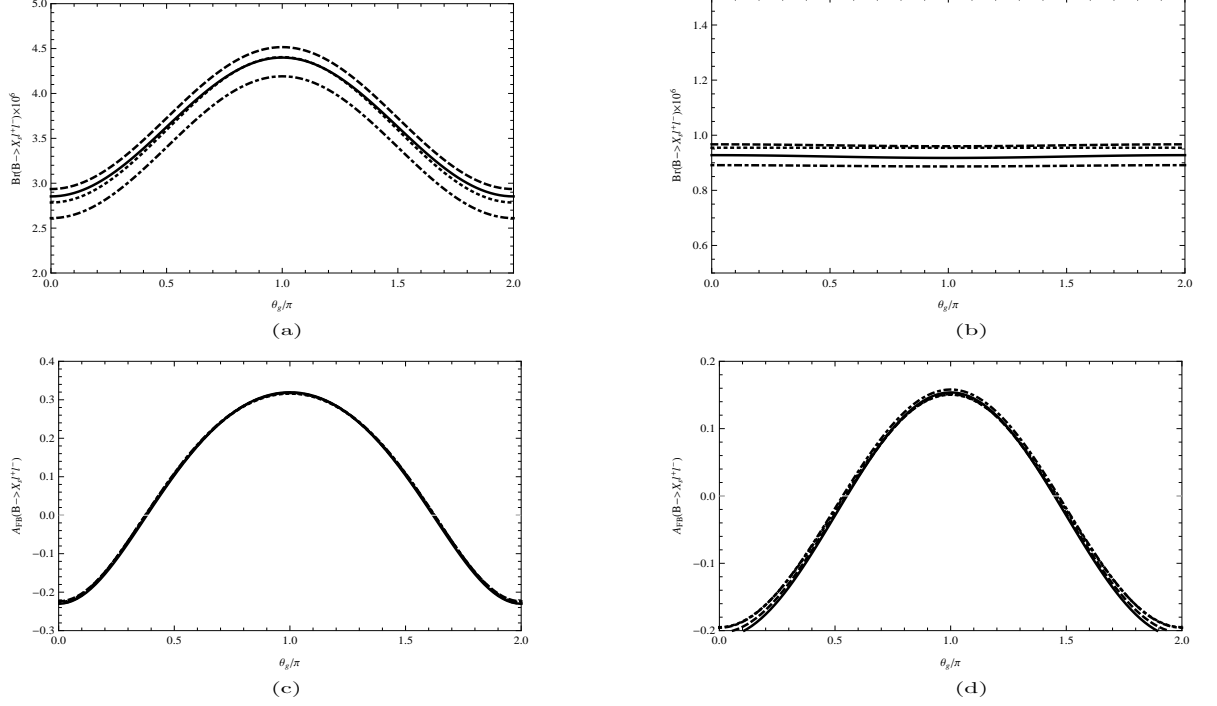


FIG. 2: Taking $(\delta_D^{LL})_{23} = (\delta_D^{RR})_{23} = (\delta_D^{LR})_{23} = 0.125$, we plot (a) $BR(B \rightarrow X_s l^+ l^-)_{q^2 \in [1,6] \text{ GeV}^2} \times 10^6$, (b) $BR(B \rightarrow X_s l^+ l^-)_{q^2 \in [14.4, 25.0] \text{ GeV}^2} \times 10^6$ (c) $A_{FB}(B \rightarrow X_s l^+ l^-)_{q^2 \in [1,6] \text{ GeV}^2}$, (d) $A_{FB}(B \rightarrow X_s l^+ l^-)_{q^2 \in [14.4, 25.0] \text{ GeV}^2}$, varying with the CP phase $\theta_{\tilde{g}}$. Where the solid lines denote $\tan \beta = 5$, dashed lines denote $\tan \beta = 10$, dotted lines denote $\tan \beta = 30$, dashed-dotted lines denote $\tan \beta = 50$, respectively.

- Taking $\tan \beta = 5$, $A_t = 1.5 \text{ TeV}$, $A_b = 1 \text{ TeV}$, $\mu = -500 \text{ GeV}$, one gets $m_h \simeq 124.6 \text{ GeV}$ correspondingly.
- Taking $\tan \beta = 10$, $A_t = 1 \text{ TeV}$, $A_b = 1 \text{ TeV}$, $\mu = 500 \text{ GeV}$, one gets $m_h \simeq 125.3 \text{ GeV}$ correspondingly.
- Taking $\tan \beta = 30$, $A_t = 0.5 \text{ TeV}$, $A_b = 1 \text{ TeV}$, $\mu = 500 \text{ GeV}$, one gets $m_h \simeq 125.2 \text{ GeV}$ correspondingly.
- Taking $\tan \beta = 50$, $A_t = .5 \text{ TeV}$, $A_b = 0.5 \text{ TeV}$, $\mu = 500 \text{ GeV}$, one gets $m_h \simeq 125.3 \text{ GeV}$ correspondingly.

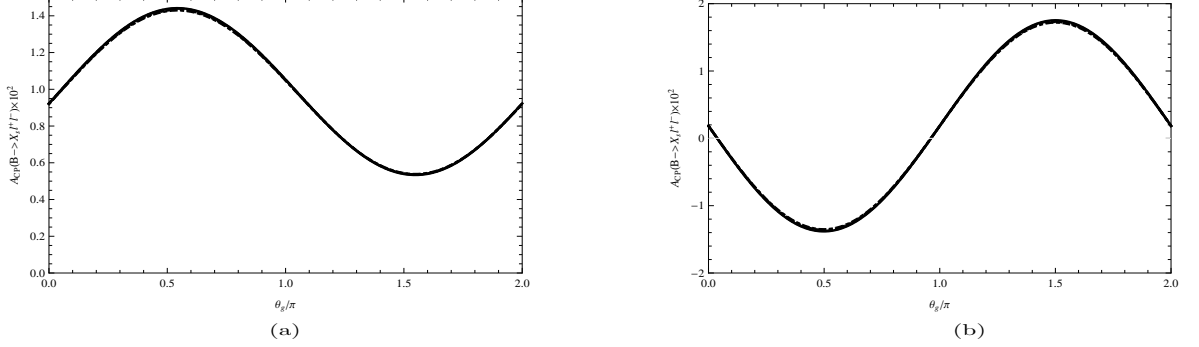


FIG. 3: Taking $(\delta_D^{LL})_{23} = (\delta_D^{RR})_{23} = (\delta_D^{LR})_{23} = 0.125$, we plot (a) $A_{CP}(B \rightarrow X_s l^+ l^-)_{q^2 \in [1, 6] \text{ GeV}^2} \times 10^2$, (b) $A_{CP}(B \rightarrow X_s l^+ l^-)_{q^2 \in [14.4, 25.0] \text{ GeV}^2} \times 10^2$, varying with the CP phase $\theta_{\tilde{g}}$. Where the solid lines denote $\tan \beta = 5$, dashed lines denote $\tan \beta = 10$, dotted lines denote $\tan \beta = 30$, dashed-dotted lines denote $\tan \beta = 50$, respectively.

For the gauge coupling of local $B - L$ symmetry and nonzero VEVs of right-handed sneutrinos, we take $g_{BL} = 0.7$, $v_N = (0, 0, 3)$ TeV here. This choice induces the mass of $U(1)_{B-L}$ gauge boson $m_{Z_{BL}} = 2.1$ TeV. Through scanning the parameter space, we find that the theoretical evaluations depend on the $U(1)_{B-L} \times U(1)_Y$ gauginos masses $|m_1|$ and $|m_{BL}|$ mildly. In our numerical analysis below, we choose $m_1 = |m_{BL}| = 1$ TeV for simplification. Furthermore, the parameter m_{1BL} only evokes the mixing between $U(1)_{B-L}$ and $U(1)_Y$ gauginos, and affects our numerical results gently. Not loss of generality, we also take $m_{1BL} = 0$ in our numerical analysis. Under the assumptions above, the numerical results are decided by the gaugino masses $|m_2|$, $|m_{\tilde{g}}|$, the CP violating phases $\theta_{\tilde{g}}$, θ_2 , θ_{BL} , and the corresponding flavor-changing insertions $(\delta_{U,D}^{LL})_{23}$, $(\delta_{U,D}^{RR})_{23}$, $(\delta_{U,D}^{LR})_{23}$.

Assuming $|m_2| = 600$ GeV, $\theta_{\tilde{g}} = \theta_2 = \theta_{BL} = 0$, we present $BR(B \rightarrow X_s l^+ l^-)_{q^2 \in [1, 6] \text{ GeV}^2} \times 10^6$ versus $|m_{\tilde{g}}|$ in Fig.1(a), $BR(B \rightarrow X_s l^+ l^-)_{q^2 \in [14.4, 25.0] \text{ GeV}^2} \times 10^6$ versus $|m_{\tilde{g}}|$ in Fig.1(b), $A_{FB}(B \rightarrow X_s l^+ l^-)_{q^2 \in [1, 6] \text{ GeV}^2}$ versus $|m_{\tilde{g}}|$ in Fig.1(c), and $A_{FB}(B \rightarrow X_s l^+ l^-)_{q^2 \in [14.4, 25.0] \text{ GeV}^2}$ versus $|m_{\tilde{g}}|$ in Fig.1(d), respectively. Since the gluino affects our numerical results through the down-type squark sector, we choose $(\delta_D^{LL})_{23} = (\delta_D^{RR})_{23} = (\delta_D^{LR})_{23} = 0.125$, $(\delta_U^{LL})_{23} = (\delta_U^{RR})_{23} = (\delta_U^{LR})_{23} = 0$ here. As $|m_{\tilde{g}}| < 1.8$ TeV, the numerical evaluations

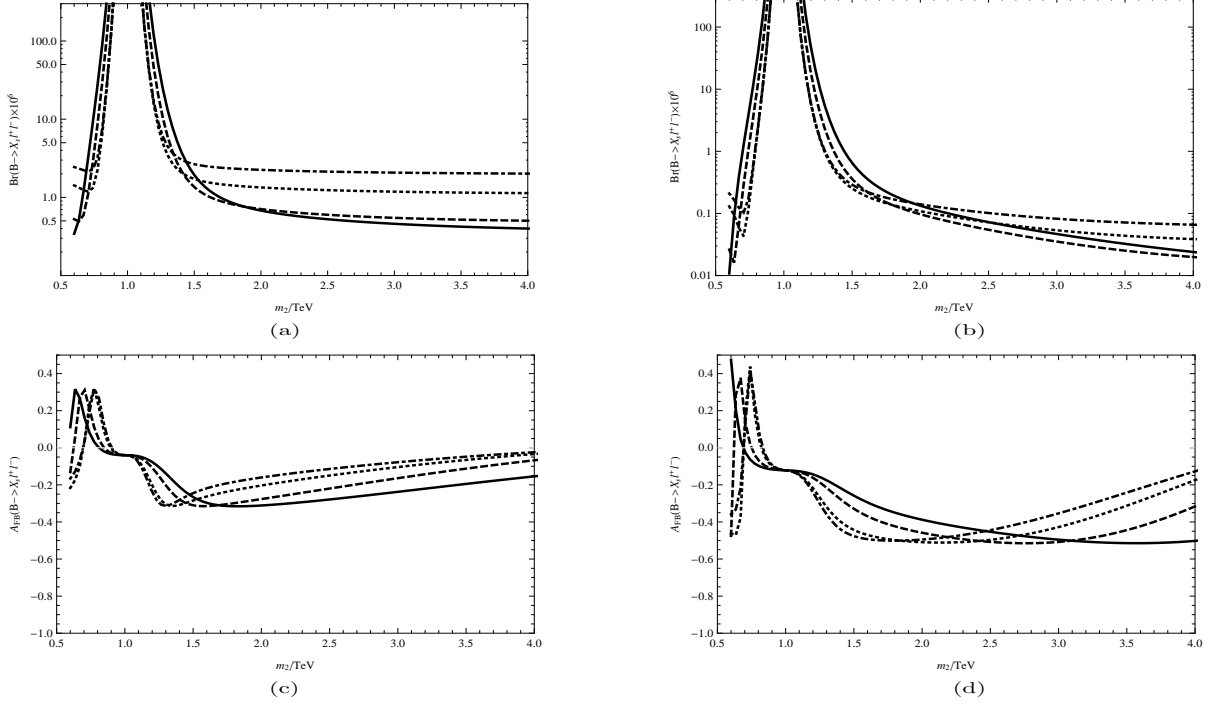


FIG. 4: Taking $(\delta_U^{LL})_{23} = (\delta_U^{RR})_{23} = (\delta_U^{LR})_{23} = 0.125$, we plot (a) $BR(B \rightarrow X_s l^+ l^-)_{q^2 \in [1, 6] \text{ GeV}^2} \times 10^6$, (b) $BR(B \rightarrow X_s l^+ l^-)_{q^2 \in [14.4, 25.0] \text{ GeV}^2} \times 10^6$ (c) $A_{FB}(B \rightarrow X_s l^+ l^-)_{q^2 \in [1, 6] \text{ GeV}^2}$, (d) $A_{FB}(B \rightarrow X_s l^+ l^-)_{q^2 \in [14.4, 25.0] \text{ GeV}^2}$, varying with the $SU(2)$ gaugino mass $|m_2|$. Where the solid lines denote $\tan \beta = 5$, dashed lines denote $\tan \beta = 10$, dotted lines denote $\tan \beta = 30$, dashed-dotted lines denote $\tan \beta = 50$, respectively.

of $BR(B \rightarrow X_s l^+ l^-)_{q^2 \in [1, 6] \text{ GeV}^2}$ exceed 2×10^{-6} . With increasing of $|m_{\tilde{g}}|$, the numerical evaluations of $BR(B \rightarrow X_s l^+ l^-)_{q^2 \in [1, 6] \text{ GeV}^2}$ decrease slowly. Meanwhile the corresponding numerical results depend on the parameter $\tan \beta$ mildly because the main corrections originate from the operators $\mathcal{O}_{7,9,10}$ in low q^2 region. Similarly the numerical evaluations of $BR(B \rightarrow X_s l^+ l^-)_{q^2 \in [14.4, 25] \text{ GeV}^2}$ exceed 0.5×10^{-6} as $|m_{\tilde{g}}| < 2 \text{ TeV}$. With increasing of $|m_{\tilde{g}}|$, the numerical evaluations of $BR(B \rightarrow X_s l^+ l^-)_{q^2 \in [14.4, 25] \text{ GeV}^2}$ decrease mildly. The corresponding numerical results depend on the parameter $\tan \beta$ subtly because the main corrections originate from the operators $\mathcal{O}_{S,P}$ in high q^2 region. In addition the numerical evaluations on A_{FB} in low q^2 region is lying in the range $-0.32 \leq A_{FB}(B \rightarrow X_s l^+ l^-)_{q^2 \in [1, 6] \text{ GeV}^2} \leq -0.18$, the numerical evaluations on A_{FB} in high q^2 region is lying in

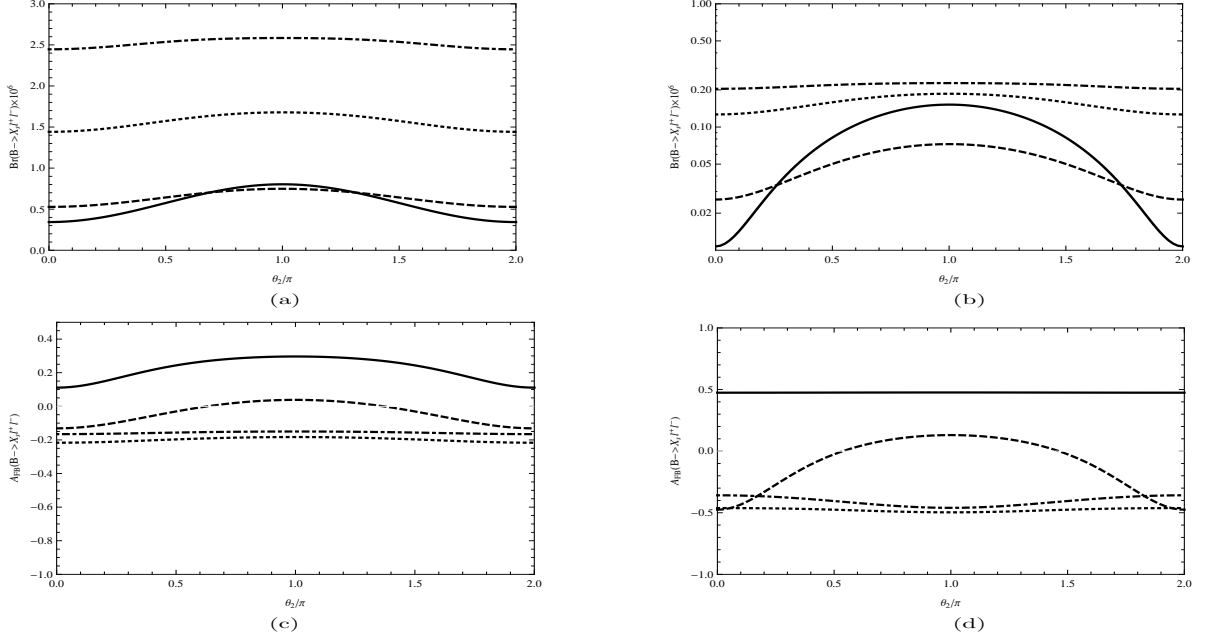


FIG. 5: Taking $(\delta_U^{LL})_{23} = (\delta_U^{RR})_{23} = (\delta_U^{LR})_{23} = 0.125$, we plot (a) $BR(B \rightarrow X_s l^+ l^-)_{q^2 \in [1, 6] \text{ GeV}^2} \times 10^6$, (b) $BR(B \rightarrow X_s l^+ l^-)_{q^2 \in [14.4, 25.0] \text{ GeV}^2} \times 10^6$ (c) $A_{FB}(B \rightarrow X_s l^+ l^-)_{q^2 \in [1, 6] \text{ GeV}^2}$, (d) $A_{FB}(B \rightarrow X_s l^+ l^-)_{q^2 \in [14.4, 25.0] \text{ GeV}^2}$, varying with the CP phase θ_2 . Where the solid lines denote $\tan \beta = 5$, dashed lines denote $\tan \beta = 10$, dotted lines denote $\tan \beta = 30$, dashed-dotted lines denote $\tan \beta = 50$, respectively.

the range $0.28 \leq A_{FB}(B \rightarrow X_s l^+ l^-)_{q^2 \in [14.4, 25.0] \text{ GeV}^2} \leq -0.18$ as $1.6 \leq |m_{\tilde{g}}|/\text{TeV} \leq 4$, which are all coincide with the experimental data within three standard deviations. Because the main corrections originate from the operators $\mathcal{O}_{S,P}$ in high q^2 region, the numerical evaluations of $A_{FB}(B \rightarrow X_s l^+ l^-)_{q^2 \in [14.4, 25.0] \text{ GeV}^2}$ depend on the parameter $\tan \beta$ subtly.

As the mass of gluino is relatively light, the CP phase of $m_{\tilde{g}}$ also affects our final result strongly. Taking $|m_2| = 600 \text{ GeV}$, $|m_{\tilde{g}}| = 1.6 \text{ TeV}$, and $\theta_2 = \theta_{BL} = 0$, we plot $BR(B \rightarrow X_s l^+ l^-)_{q^2 \in [1, 6] \text{ GeV}^2} \times 10^6$ varying with $\theta_{\tilde{g}}$ in Fig.2(a), $BR(B \rightarrow X_s l^+ l^-)_{q^2 \in [14.4, 25.0] \text{ GeV}^2} \times 10^6$ varying with $\theta_{\tilde{g}}$ in Fig.2(b), $A_{FB}(B \rightarrow X_s l^+ l^-)_{q^2 \in [1, 6] \text{ GeV}^2}$ varying with $\theta_{\tilde{g}}$ in Fig.2(c), and $A_{FB}(B \rightarrow X_s l^+ l^-)_{q^2 \in [14.4, 25.0] \text{ GeV}^2}$ varying with $\theta_{\tilde{g}}$ in Fig.2(d), respectively. In low q^2 region, the theoretical prediction on $BR(B \rightarrow X_s l^+ l^-)_{q^2 \in [1, 6] \text{ GeV}^2}$ increases from 2.5×10^{-6} to $4.5 \times$

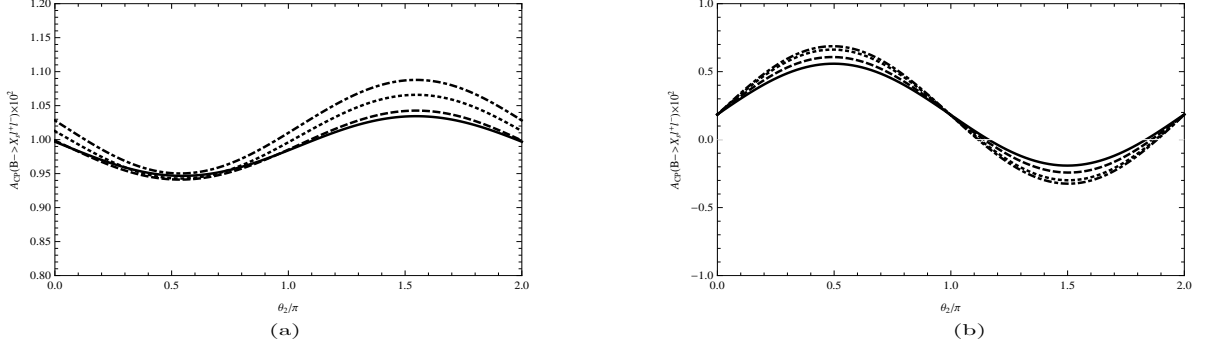


FIG. 6: Taking $(\delta_U^{LL})_{23} = (\delta_U^{RR})_{23} = (\delta_U^{LR})_{23} = 0.125$, we plot (a) $A_{CP}(B \rightarrow X_s l^+ l^-)_{q^2 \in [1, 6] \text{ GeV}^2} \times 10^2$, (b) $A_{CP}(B \rightarrow X_s l^+ l^-)_{q^2 \in [14.4, 25.0] \text{ GeV}^2} \times 10^2$, varying with the CP phase θ_2 . Where the solid lines denote $\tan \beta = 5$, dashed lines denote $\tan \beta = 10$, dotted lines denote $\tan \beta = 30$, dashed-dotted lines denote $\tan \beta = 50$, respectively.

10^{-6} as the CP phase $\theta_{\tilde{g}}$ increases from 0 to π , and the forward-backward asymmetry $A_{FB}(B \rightarrow X_s l^+ l^-)_{q^2 \in [1, 6] \text{ GeV}^2}$ changes from -0.2 to 0.3 when the CP phase $\theta_{\tilde{g}}$ increases from 0 to π , respectively. In high q^2 region, the branching ratio $BR(B \rightarrow X_s l^+ l^-)_{q^2 \in [14.4, 25.0] \text{ GeV}^2}$ varies mildly with increasing of the CP phase $\theta_{\tilde{g}}$ because the corrections from the operators $\mathcal{O}_{S,P}$ are important in this region. Nevertheless $A_{FB}(B \rightarrow X_s l^+ l^-)_{q^2 \in [14.4, 25] \text{ GeV}^2}$ changes from -0.2 to 0.18 when the CP phase $\theta_{\tilde{g}}$ increases from 0 to π .

Using the inputs presented in Table.(II), one gets the SM predictions on the CP asymmetries as $A_{CP}(B \rightarrow X_s l^+ l^-)_{q^2 \in [1, 6] \text{ GeV}^2} \sim 10^{-3}$, $A_{CP}(B \rightarrow X_s l^+ l^-)_{q^2 \in [14.4, 25] \text{ GeV}^2} < 10^{-4}$, respectively. Taking $(\delta_D^{LL})_{23} = (\delta_D^{RR})_{23} = (\delta_D^{LR})_{23} = 0.125$, we plot $A_{CP}(B \rightarrow X_s l^+ l^-)_{q^2 \in [1, 6] \text{ GeV}^2} \times 10^2$ versus $\theta_{\tilde{g}}$ in Fig.3(a), $A_{CP}(B \rightarrow X_s l^+ l^-)_{q^2 \in [14.4, 25.0] \text{ GeV}^2} \times 10^2$, versus the CP phase $\theta_{\tilde{g}}$ in Fig.3(b). Where the solid lines denote $\tan \beta = 5$, dashed lines denote $\tan \beta = 10$, dotted lines denote $\tan \beta = 30$, dashed-dotted lines denote $\tan \beta = 50$, respectively. The CP asymmetry $A_{CP}(B \rightarrow X_s l^+ l^-)_{q^2 \in [1, 6] \text{ GeV}^2}$ reaches 1.4% as $\theta_{\tilde{g}} = \pi/2$, the CP asymmetry $A_{CP}(B \rightarrow X_s l^+ l^-)_{q^2 \in [14.4, 25] \text{ GeV}^2}$ changes from -1.2% to 1.8% when the CP phase $\theta_{\tilde{g}}$ varies from $\pi/2$ to $3\pi/2$. We anticipate that the CP asymmetries exceeding 0.01 can be detected in near future.

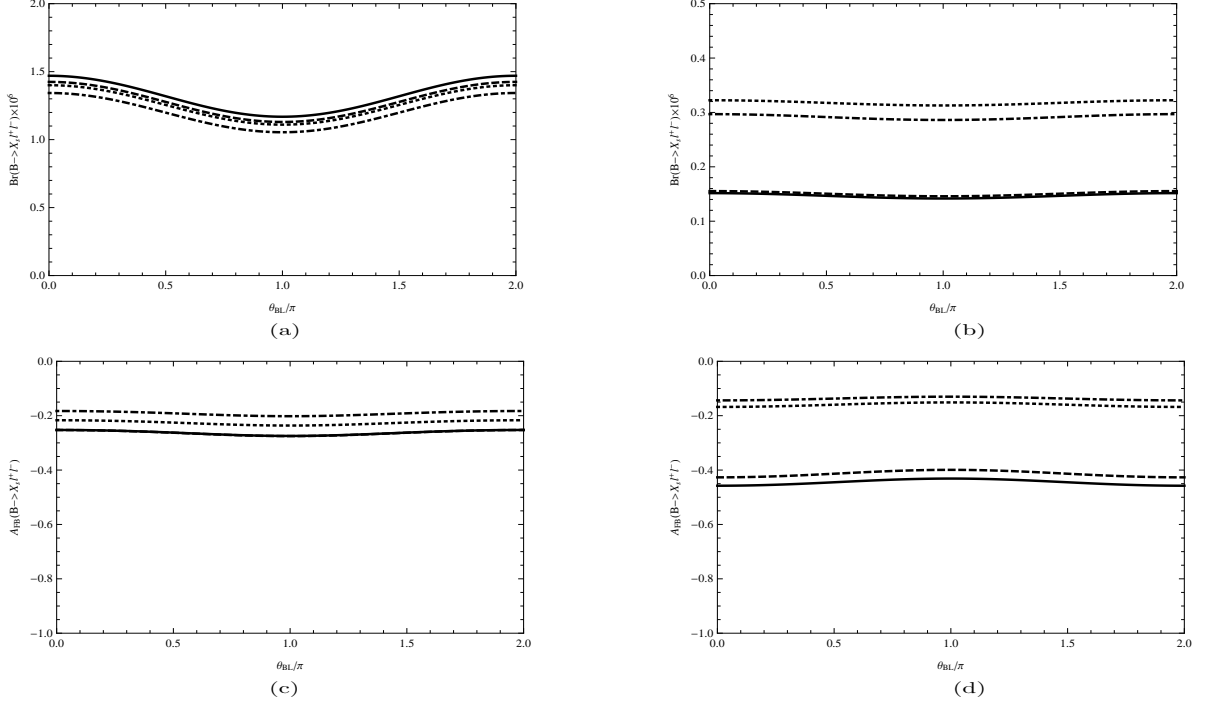


FIG. 7: Taking $(\delta_D^{LL})_{23} = (\delta_D^{RR})_{23} = (\delta_D^{LR})_{23} = 0.125$, we plot (a) $BR(B \rightarrow X_s l^+ l^-)_{q^2 \in [1, 6] \text{ GeV}^2} \times 10^6$, (b) $BR(B \rightarrow X_s l^+ l^-)_{q^2 \in [14.4, 25.0] \text{ GeV}^2} \times 10^6$ (c) $A_{FB}(B \rightarrow X_s l^+ l^-)_{q^2 \in [1, 6] \text{ GeV}^2}$, (d) $A_{FB}(B \rightarrow X_s l^+ l^-)_{q^2 \in [14.4, 25.0] \text{ GeV}^2}$, varying with the CP phase $\theta_{\tilde{g}}$. Where the solid lines denote $\tan \beta = 5$, dashed lines denote $\tan \beta = 10$, dotted lines denote $\tan \beta = 30$, dashed-dotted lines denote $\tan \beta = 50$, respectively.

To investigate the corrections from chargino sector, we choose $(\delta_D^{LL})_{23} = (\delta_D^{RR})_{23} = (\delta_D^{LR})_{23} = 0$, and $|m_{\tilde{g}}| = 4 \text{ TeV}$ to suppress the contributions from gluinos and down-type squarks. So far the experimental data do not exclude relatively light neutralinos and charginos with several hundred GeV masses yet. Assuming $\theta_{\tilde{g}} = \theta_2 = \theta_{BL} = 0$, and the insertions $(\delta_U^{LL})_{23} = (\delta_U^{RR})_{23} = (\delta_U^{LR})_{23} = 0.125$, we present $BR(B \rightarrow X_s l^+ l^-)_{q^2 \in [1, 6] \text{ GeV}^2} \times 10^6$ versus the $SU(2)$ gaugino mass $|m_2|$ in Fig.3(a), $BR(B \rightarrow X_s l^+ l^-)_{q^2 \in [14.4, 25.0] \text{ GeV}^2} \times 10^6$ versus the $SU(2)$ gaugino mass $|m_2|$ in Fig.3(b), $A_{FB}(B \rightarrow X_s l^+ l^-)_{q^2 \in [1, 6] \text{ GeV}^2}$ versus the $SU(2)$ gaugino mass $|m_2|$ in Fig.3(c), and $A_{FB}(B \rightarrow X_s l^+ l^-)_{q^2 \in [14.4, 25.0] \text{ GeV}^2}$ versus the $SU(2)$ gaugino mass $|m_2|$ in Fig.3(d), respectively. As $|m_2| > 2 \text{ TeV}$, $BR(B \rightarrow X_s l^+ l^-)_{q^2 \in [1, 6] \text{ GeV}^2}$ and $BR(B \rightarrow X_s l^+ l^-)_{q^2 \in [14.4, 25] \text{ GeV}^2}$ both coincide with the experimental data in three standard

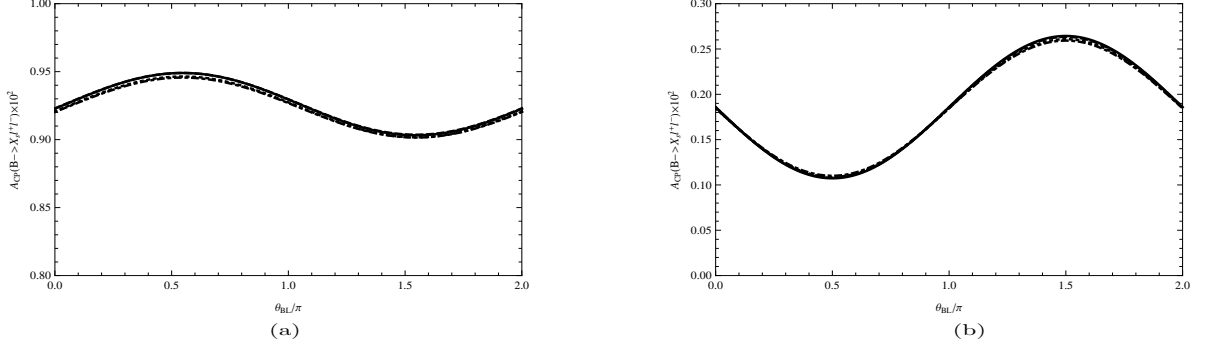


FIG. 8: Taking $(\delta_D^{LL})_{23} = (\delta_D^{RR})_{23} = (\delta_D^{LR})_{23} = 0.125$, we plot (a) $A_{CP}(B \rightarrow X_s l^+ l^-)_{q^2 \in [1, 6] \text{ GeV}^2} \times 10^2$, (b) $A_{CP}(B \rightarrow X_s l^+ l^-)_{q^2 \in [14.4, 25.0] \text{ GeV}^2} \times 10^2$, varying with the CP phase θ_{BL} . Where the solid lines denote $\tan \beta = 5$, dashed lines denote $\tan \beta = 10$, dotted lines denote $\tan \beta = 30$, dashed-dotted lines denote $\tan \beta = 50$, respectively.

deviations. The resonance peaks around 1 TeV originate from the box diagrams involving sleptons/sneutrinos and neutralinos/charginos under our assumptions on parameter space. As $|m_2| = 1.5$ TeV, the numerical evaluation on $A_{FB}(B \rightarrow X_s l^+ l^-)_{q^2 \in [1, 6] \text{ GeV}^2}$ is about -0.4 , and increases slowly with increasing of $|m_2|$. In high q^2 region the corrections from the operators $\mathcal{O}_{S,P}$ affect our numerical results heavily. As $|m_2| = 2.5$ TeV, the numerical result indicates $A_{FB}(B \rightarrow X_s l^+ l^-)_{q^2 \in [14.4, 25] \text{ GeV}^2} \simeq -0.5$. Along with increasing of $|m_2|$, the numerical evaluations on $A_{FB}(B \rightarrow X_s l^+ l^-)_{q^2 \in [14.4, 25] \text{ GeV}^2}$ of $\tan \beta = 50$ are faster than those of lower of $\tan \beta$.

Under our assumptions on the parameter space, there is a relatively light chargino with mass in the range $500 \text{ GeV} \leq m_{\tilde{\chi}_1^\pm} \leq 1 \text{ TeV}$. Therefore the CP phase of m_2 also affects our numerical results. Taking $|m_2| = 600 \text{ GeV}$, $|m_{\tilde{g}}| = 4 \text{ TeV}$, and $\theta_{\tilde{g}} = \theta_{BL} = 0$, we present $BR(B \rightarrow X_s l^+ l^-)_{q^2 \in [1, 6] \text{ GeV}^2} \times 10^6$ versus θ_2 in Fig.5(a), $BR(B \rightarrow X_s l^+ l^-)_{q^2 \in [14.4, 25.0] \text{ GeV}^2} \times 10^6$ versus θ_2 in Fig.5(b), $A_{FB}(B \rightarrow X_s l^+ l^-)_{q^2 \in [1, 6] \text{ GeV}^2}$ versus θ_2 in Fig.5(c), and $A_{FB}(B \rightarrow X_s l^+ l^-)_{q^2 \in [14.4, 25.0] \text{ GeV}^2}$ versus θ_2 in Fig.5(d), respectively. When $\tan \beta = 5$ and $\pi/2 \leq \theta_2 \leq 3\pi/2$, we get $0.4 \times 10^{-6} \leq BR(B \rightarrow X_s l^+ l^-)_{q^2 \in [1, 6] \text{ GeV}^2} \leq 0.8 \times 10^{-6}$, $0.07 \times 10^{-6} \leq BR(B \rightarrow X_s l^+ l^-)_{q^2 \in [14.4, 25] \text{ GeV}^2} \leq 0.12 \times 10^{-6}$ respectively, which

coincide with the experimental data in 3σ permissions. As $\tan\beta = 10$, one finds the numerical evaluations of $BR(B \rightarrow X_s l^+ l^-)_{q^2 \in [1,6] \text{ GeV}^2}$ satisfying the experimental constraint within three standard deviations. However the choice of $\tan\beta = 10$ is excluded by experimental observations because $0.02 \times 10^{-6} \leq BR(B \rightarrow X_s l^+ l^-)_{q^2 \in [14.4, 25] \text{ GeV}^2} \leq 0.05 \times 10^{-6}$, which does not satisfy the experimental data in 3 standard deviations. For large $\tan\beta = 30, 50$, the corrections from the operators $\mathcal{O}_{s,P}$ are enhanced drastically. Correspondingly the theoretical predictions on the branching ratios in low and high q^2 regions all coincide with the experimental data, respectively. The forward-backward asymmetries both in low and high q^2 regions depend on the CP phase θ_2 smoothly, the absolute values of corresponding evaluations exceed 0.05 which can be detected in future.

As mentioned above, the SM predictions on the CP asymmetries are $A_{CP}(B \rightarrow X_s l^+ l^-)_{q^2 \in [1,6] \text{ GeV}^2} \sim 10^{-3}$, $A_{CP}(B \rightarrow X_s l^+ l^-)_{q^2 \in [14.4, 25] \text{ GeV}^2} < 10^{-4}$, which are difficult to detected in near future. Taking $(\delta_U^{LL})_{23} = (\delta_U^{RR})_{23} = (\delta_U^{LR})_{23} = 0.125$, we plot $A_{CP}(B \rightarrow X_s l^+ l^-)_{q^2 \in [1,6] \text{ GeV}^2} \times 10^2$ varying with θ_2 in Fig.6(a), $A_{CP}(B \rightarrow X_s l^+ l^-)_{q^2 \in [14.4, 25.0] \text{ GeV}^2} \times 10^2$, varying with the CP phase θ_2 in Fig.6(b), respectively. Assuming that the CP violation originates from CKM in the SM, one finds $A_{CP}(B \rightarrow X_s l^+ l^-)_{q^2 \in [1,6] \text{ GeV}^2} \sim 0.01$, $A_{CP}(B \rightarrow X_s l^+ l^-)_{q^2 \in [14.4, 25] \text{ GeV}^2} \sim 0.002$, respectively. The theoretical predictions of $A_{CP}(B \rightarrow X_s l^+ l^-)_{q^2 \in [1,6] \text{ GeV}^2}$ depends on θ_2 gently. Nevertheless, the new CP phase θ_2 modifies numerical results of $A_{CP}(B \rightarrow X_s l^+ l^-)_{q^2 \in [14.4, 25.0] \text{ GeV}^2}$ strongly.

When $(\delta_U^{LL})_{23} = (\delta_U^{RR})_{23} = (\delta_U^{LR})_{23} = 0$, and $(\delta_D^{LL})_{23} = (\delta_D^{RR})_{23} = (\delta_D^{LR})_{23} \neq 0$, the $SU(2)$ gaugino mass m_2 and $U(1)$ gaugino mass m_1 affect our numerical results through the mixing matrix of neutralinos. The numerical evaluations indicate that those physics quantities depend on m_2, m_1 mildly in the sectors of parameter space. Similarly the $U(1)_{B-L}$ gaugino mass $|m_{BL}|$ also affects our results gently.

Under our assumptions on the parameter space, it is interesting to investigate the effect of CP phase θ_{BL} on our numerical analyses. Taking $(\delta_D^{LL})_{23} = (\delta_D^{RR})_{23} = (\delta_D^{LR})_{23} = 0.125$, $(\delta_U^{LL})_{23} = (\delta_U^{RR})_{23} = (\delta_U^{LR})_{23} = 0$, $|m_2| = 600 \text{ GeV}$, $|m_{\tilde{g}}| = 4 \text{ TeV}$, and $\theta_{\tilde{g}} = \theta_2 = 0$, we present $BR(B \rightarrow X_s l^+ l^-)_{q^2 \in [1,6] \text{ GeV}^2} \times 10^6$ versus θ_{BL} in Fig.7(a), $BR(B \rightarrow X_s l^+ l^-)_{q^2 \in [14.4, 25.0] \text{ GeV}^2} \times 10^6$ versus θ_{BL} in Fig.7(b), $A_{FB}(B \rightarrow X_s l^+ l^-)_{q^2 \in [1,6] \text{ GeV}^2}$ versus θ_2 in Fig.7(c), and $A_{FB}(B \rightarrow X_s l^+ l^-)_{q^2 \in [14.4, 25.0] \text{ GeV}^2}$ versus θ_{BL} in Fig.5(d), respectively. Our theo-

retical evaluations depend on the CP phase θ_{BL} slowly. The numerical results on branching ratios in low q^2 and high q^2 regions satisfy the experimental data simultaneously in three standard permissions. $A_{FB}(B \rightarrow X_s l^+ l^-)_{q^2 \in [1,6] \text{ GeV}^2} \sim -0.2$ for all $\tan \beta$ chosen. As $\tan \beta = 5, 10$, $A_{FB}(B \rightarrow X_s l^+ l^-)_{q^2 \in [14.4, 25.0] \text{ GeV}^2} \sim -0.4$, and $A_{FB}(B \rightarrow X_s l^+ l^-)_{q^2 \in [14.4, 25.0] \text{ GeV}^2} \sim -0.2$ as $\tan \beta = 30, 50$. Additionally we present $A_{CP}(B \rightarrow X_s l^+ l^-)_{q^2 \in [1,6] \text{ GeV}^2} \times 10^2$ varying with θ_{BL} in Fig.8(a), $A_{CP}(B \rightarrow X_s l^+ l^-)_{q^2 \in [14.4, 25.0] \text{ GeV}^2} \times 10^2$, varying with the CP phase θ_{BL} in Fig.8(b), respectively. Assuming that the CP violation originates from CKM matrix elements, one finds $A_{CP}(B \rightarrow X_s l^+ l^-)_{q^2 \in [1,6] \text{ GeV}^2} \sim 0.01$, $A_{CP}(B \rightarrow X_s l^+ l^-)_{q^2 \in [14.4, 25] \text{ GeV}^2} \sim 0.002$, respectively. The theoretical predictions of $A_{CP}(B \rightarrow X_s l^+ l^-)_{q^2 \in [1,6] \text{ GeV}^2}$ depends on θ_{BL} gently. Nevertheless, the new CP phase θ_{BL} modifies numerical results of $A_{CP}(B \rightarrow X_s l^+ l^-)_{q^2 \in [14.4, 25.0] \text{ GeV}^2}$ strongly.

In our assumptions on parameter space, the theoretical predictions on $Br(\bar{B} \rightarrow X_s \gamma)$ and $Br(B_s \rightarrow \mu^+ \mu^-)$ all coincide with the experimental observations in three standard permissions. Obviously our numerical results on branching ratios, forward-backward asymmetries, and CP asymmetries in $B \rightarrow X_s l^+ l^-$ depend on the mass insertions $(\delta_{U,D}^{LL})_{23}$, $(\delta_{U,D}^{RR})_{23}$, $(\delta_{U,D}^{LR})_{23}$ and corresponding CP phases subtly. Here we do not present theoretical evaluations on above quantities versus mass insertions explicitly, because some similar analyses are given in our previous works[39, 56]. In addition we take a relatively small coupling of $U(1)_{B-L}$ as $g_{BL} \leq g_2$, this choice avoid the Landau pole of g_{BL} below the energy scale of grand unified theories.

VI. SUMMARY

Rare B -meson decays are very sensitive to new physics beyond the SM since the theoretical evaluations on corresponding physical quantities are not seriously affected by the uncertainties originating from unperturbative QCD effects. Considering the constraint from the observed Higgs signal at the LHC, we study the supersymmetric corrections to the branching ratios $BR(B \rightarrow X_s l^+ l^-)$, ($l = e, \mu$) in the MSSM with local $U(1)_{B-L}$ symmetry[47–50] with nonuniversal soft breaking terms. After obtaining the Wilson coefficients at matching scale, we evolve the Wilson coefficients from the SM down to hadronic

scale at NNLL accuracy, and evolve that from new physics down to hadronic scale at LL accuracy, respectively. The lightest neutral Higgs with mass around 125 GeV constrains the correlation between $\tan\beta$ and the soft Yukawa coupling A_t , A_b strongly, nevertheless constrains neutral flavor changing mass insertions weakly. Under our assumptions on parameters of the considered model, the numerical analyses indicate that the branching ratios, and forward-backward asymmetries depend on the gaugino masses $m_{\tilde{g}}$, m_2 strongly, new possible CP phases can enhance the CP asymmetries exceed 1%, which can be detected in near future.

Acknowledgments

The work has been supported by the National Natural Science Foundation of China (NNSFC) with Grant No. 11275036, and No. 11535002, the Open Project Program of State Key Laboratory of Theoretical Physics, Institute of Theoretical Physics, Chinese Academy of Sciences, China(No.Y5KF131CJ1), the Natural Science Foundation of Hebei province with Grant No. A2013201277, No. A2016201010, No. A2016201069, and Natural Science Foundation of Hebei University with Grant No. 2011JQ05, No. 2012-242.

Appendix A: The mass squared matrices for squarks

With the minimal flavor violation assumption, the 2×2 mass squared matrix for scalar tops is given as

$$\mathcal{Z}_t^\dagger \begin{pmatrix} m_{\tilde{t}_L}^2 & m_{\tilde{t}_X}^2 \\ m_{\tilde{t}_X}^2 & m_{\tilde{t}_R}^2 \end{pmatrix} \mathcal{Z}_t = \text{diag}(m_{\tilde{t}_1}^2, m_{\tilde{t}_2}^2), \quad (\text{A1})$$

with

$$m_{\tilde{t}_L}^2 = \frac{(g_1^2 + g_2^2)v_{\text{EW}}^2}{24}(1 - 2\cos^2\beta)(1 - 4c_w^2) + \frac{g_{BL}^2}{6}(v_N^2 - v_{\text{EW}}^2 + v_{\text{SM}}^2) + m_t^2 + m_{\tilde{Q}_3}^2,$$

$$\begin{aligned}
m_{\tilde{t}_R}^2 &= -\frac{g_1^2 v_{\text{EW}}^2}{6} (1 - 2 \cos^2 \beta) \\
&\quad - \frac{g_{BL}^2}{6} (v_N^2 - v_{\text{EW}}^2 + v_{\text{SM}}^2) + m_t^2 + m_{\tilde{U}_3}^2, \\
m_{\tilde{t}_X}^2 &= -\frac{v_u}{\sqrt{2}} A_t Y_t + \frac{\mu v_d}{\sqrt{2}} Y_t.
\end{aligned} \tag{A2}$$

Here Y_t , A_t denote Yukawa coupling and trilinear soft-breaking parameters in top quark sector, respectively. In a similar way, the mass-squared matrix for scalar bottoms is

$$\mathcal{Z}_b^\dagger \begin{pmatrix} m_{\tilde{b}_L}^2 & m_{\tilde{b}_X}^2 \\ m_{\tilde{b}_X}^2 & m_{\tilde{b}_R}^2 \end{pmatrix} \mathcal{Z}_b = \text{diag}(m_{\tilde{b}_1}^2, m_{\tilde{b}_2}^2), \tag{A3}$$

with

$$\begin{aligned}
m_{\tilde{b}_L}^2 &= \frac{(g_1^2 + g_2^2) v_{\text{EW}}^2}{24} (1 - 2 \cos^2 \beta) (1 + 2c_w^2) \\
&\quad + \frac{g_{BL}^2}{6} (v_N^2 - v_{\text{EW}}^2 + v_{\text{SM}}^2) + m_b^2 + m_{\tilde{Q}_3}^2, \\
m_{\tilde{b}_R}^2 &= \frac{g_1^2 v_{\text{EW}}^2}{12} (1 - 2 \cos^2 \beta) \\
&\quad - \frac{g_{BL}^2}{6} (v_N^2 - v_{\text{EW}}^2 + v_{\text{SM}}^2) + m_b^2 + m_{\tilde{D}_3}^2, \\
m_{\tilde{b}_X}^2 &= \frac{v_d}{\sqrt{2}} A_b Y_b - \frac{\mu v_u}{\sqrt{2}} Y_b,
\end{aligned} \tag{A4}$$

here Y_b , A_b denote Yukawa couplings and trilinear soft-breaking parameters in B quark sector, respectively.

Appendix B: The Wilson coefficients from $U(1)_{B-L}$ interaction at electroweak scale

Adopting mass insertion approximation, we present the corrections to those Wilson coefficients from $U(1)_{B-L}$ interaction here

$$\begin{aligned}
C_{9, \tilde{Z}_{BL}}^\gamma(\mu_{\text{EW}}) &= \frac{Q_d \alpha_s(\mu_{\text{EW}}) \alpha_{BL} s_W^2}{324 \pi \alpha_{\text{EW}}(\mu_{\text{EW}})} \frac{(\delta^2 m_{\tilde{D}}^{LL})_{23}}{\Lambda_{NP}^2 V_{tb} V_{ts}^*} x_W T_3(x_{\tilde{Z}_{BL}}, x_{\tilde{b}_L}, x_{\tilde{s}_L}) \\
&\quad - \frac{Q_d \alpha_s(\mu_{\text{EW}}) \alpha_{BL} s_W^2}{324 \pi \alpha_{\text{EW}}(\mu_{\text{EW}})} \frac{(\delta^2 m_{\tilde{D}}^{LR})_{23} (\delta^2 m_{\tilde{D}}^{LR})_{33}^*}{\Lambda_{NP}^4 V_{tb} V_{ts}^*} x_W D_3(x_{\tilde{Z}_{BL}}, x_{\tilde{b}_L}, x_{\tilde{b}_R}, x_{\tilde{s}_L}),
\end{aligned}$$

$$\begin{aligned}
C_{10,\tilde{Z}_{BL}}^Z(\mu_{EW}) &= \frac{\alpha_s(\mu_{EW})\alpha_{BL}}{144\pi\alpha_{EW}(\mu_{EW})} \left(1 - \frac{2}{3}s_W^2\right) \frac{(\delta^2 m_{\tilde{D}}^{LL})_{23}}{\Lambda_{NP}^2 V_{tb} V_{ts}^*} \left[T_B - \frac{\partial \varrho_{2,1}}{\partial x_{\tilde{s}_L}} - \frac{\partial \varrho_{2,1}}{\partial x_{\tilde{b}_L}}\right] (x_{\tilde{Z}_{BL}}, x_{\tilde{b}_L}, x_{\tilde{s}_L}) \\
&\quad - \frac{\alpha_s(\mu_{EW})\alpha_{BL}}{144\pi\alpha_{EW}(\mu_{EW})} \frac{(\delta^2 m_{\tilde{D}}^{LR})_{23} (\delta^2 m_{\tilde{D}}^{LR})_{33}^*}{\Lambda_{NP}^4 V_{tb} V_{ts}^*} \left[\left(1 - \frac{2}{3}s_W^2\right) \left(D_B - \frac{\partial \varrho_{2,1}}{\partial x_{\tilde{s}_L}} - \frac{\partial \varrho_{2,1}}{\partial x_{\tilde{b}_L}}\right) \right. \\
&\quad \left. - \frac{2}{3}s_W^2 \frac{\partial \varrho_{2,1}}{\partial x_{\tilde{b}_L}}\right] (x_{\tilde{Z}_{BL}}, x_{\tilde{b}_L}, x_{\tilde{b}_R}, x_{\tilde{s}_L}), \\
C_{9,H^\pm}^{Z_{BL}}(\mu_{EW}) &= \frac{\alpha_s(\mu_{EW})\alpha_{BL}}{24\pi\alpha_{EW}(\mu_{EW})s_W^2} \frac{x_W}{x_{Z_{BL}}} \left\{ \left[-1 - 2\varrho_{1,1} + 2x_t \frac{\partial \varrho_{1,1}}{\partial x_t} \right] (x_t, x_W) \right. \\
&\quad \left. + \frac{x_t}{x_W s_\beta^2} \sum_{i=1}^2 (Z_{H^\pm})_{1i} (Z_{H^\pm})_{1i}^* \left[-3 + 2\varrho_{1,1} - 2 \frac{\partial \varrho_{2,1}}{\partial x_t} + 2x_t \frac{\partial \varrho_{1,1}}{\partial x_t} \right] (x_t, x_{H_i^\pm}) \right\}, \\
C_{9,\chi^\pm}^{Z_{BL}}(\mu_{EW}) &= -\frac{\alpha_s(\mu_{EW})\alpha_{BL}}{24\pi\alpha_{EW}(\mu_{EW})} \frac{(\delta^2 m_{\tilde{U}}^{LL})_{23}}{\Lambda_{NP}^2 V_{tb} V_{ts}^*} (U_+)^*_{1i} (U_+)_{1i} \frac{x_W}{x_{Z_{BL}}} (T_B - 2T_{BL}) (x_{\chi_i^\pm}, x_{\tilde{t}_L}, x_{\tilde{c}_L}) \\
&\quad + \frac{\alpha_s(\mu_{EW})\alpha_{BL}m_t}{24\pi\alpha_{EW}(\mu_{EW})m_W s_\beta} \frac{(\delta^2 m_{\tilde{U}}^{LR})_{23}}{\Lambda_{NP}^2 V_{tb} V_{ts}^*} (U_+)^*_{1i} (U_+)_{2i} \frac{x_W}{x_{Z_{BL}}} (T_B - 2T_{BL}) (x_{\chi_i^\pm}, x_{\tilde{t}_R}, x_{\tilde{c}_L}) \\
&\quad + \frac{\alpha_s(\mu_{EW})\alpha_{BL}}{24\pi\alpha_{EW}(\mu_{EW})} \frac{(\delta^2 m_{\tilde{U}}^{LL})_{23} (\delta^2 m_{\tilde{U}}^{LR})_{33}^*}{\Lambda_{NP}^4 V_{tb} V_{ts}^*} (U_+)^*_{1i} (U_+)_{1i} \frac{x_W}{x_{Z_{BL}}} \\
&\quad \times (D_B - 2D_{BL}) (x_{\chi_i^\pm}, x_{\tilde{t}_L}, x_{\tilde{t}_R}, x_{\tilde{c}_L}) \\
&\quad - \frac{\alpha_s(\mu_{EW})\alpha_{BL}m_t}{24\pi\alpha_{EW}(\mu_{EW})m_W s_\beta} \frac{(\delta^2 m_{\tilde{U}}^{LR})_{23} (\delta^2 m_{\tilde{U}}^{LR})_{33}^*}{\Lambda_{NP}^4 V_{tb} V_{ts}^*} (U_+)^*_{1i} (U_+)_{2i} \frac{x_W}{x_{Z_{BL}}} \\
&\quad \times (D_B - 2D_{BL}) (x_{\chi_i^\pm}, x_{\tilde{t}_R}, x_{\tilde{t}_L}, x_{\tilde{c}_L}), \\
C_{9,\chi^0}^{Z_{BL}}(\mu_{EW}) &= -\frac{\alpha_s(\mu_{EW})\alpha_{BL}}{24\pi\alpha_{EW}(\mu_{EW})c_W^2} \frac{(\delta^2 m_{\tilde{D}}^{LL})_{23}}{\Lambda_{NP}^2 V_{tb} V_{ts}^*} |\mathcal{N}_d^i|^2 \frac{x_W}{x_{Z_{BL}}} (T_B - \frac{1}{2}T_{BL}) (x_{\chi_i^0}, x_{\tilde{b}_L}, x_{\tilde{s}_L}) \\
&\quad - \frac{\alpha_s(\mu_{EW})\alpha_{BL}m_b m_s}{24\pi\alpha_{EW}(\mu_{EW})m_W^2 c_\beta^2} \frac{(\delta^2 m_{\tilde{D}}^{RR})_{23}}{\Lambda_{NP}^2 V_{tb} V_{ts}^*} |(U_N)_{3i}|^2 \frac{x_W}{x_{Z_{BL}}} (T_B - \frac{1}{2}T_{BL}) (x_{\chi_i^0}, x_{\tilde{b}_R}, x_{\tilde{s}_R}) \\
&\quad - \frac{\alpha_s(\mu_{EW})\alpha_{BL}m_b}{24\pi\alpha_{EW}(\mu_{EW})m_W c_W c_\beta} \frac{(\delta^2 m_{\tilde{D}}^{LR})_{23}}{\Lambda_{NP}^2 V_{tb} V_{ts}^*} (U_N)_{3i} \mathcal{N}_d^{i*} \frac{x_W}{x_{Z_{BL}}} (T_B - \frac{1}{2}T_{BL}) (x_{\chi_i^0}, x_{\tilde{b}_R}, x_{\tilde{s}_L}) \\
&\quad - \frac{\alpha_s(\mu_{EW})\alpha_{BL}m_s}{24\pi\alpha_{EW}(\mu_{EW})m_W c_W c_\beta} \frac{(\delta^2 m_{\tilde{D}}^{LR})_{23}}{\Lambda_{NP}^2 V_{tb} V_{ts}^*} (U_N)^*_{3i} \mathcal{N}_d^i \frac{x_W}{x_{Z_{BL}}} (T_B - \frac{1}{2}T_{BL}) (x_{\chi_i^0}, x_{\tilde{b}_L}, x_{\tilde{s}_R}) \\
&\quad + \frac{\alpha_s(\mu_{EW})\alpha_{BL}}{24\pi\alpha_{EW}(\mu_{EW})c_W^2} \frac{(\delta^2 m_{\tilde{D}}^{LR})_{23} (\delta^2 m_{\tilde{D}}^{LR})_{33}^*}{\Lambda_{NP}^4 V_{tb} V_{ts}^*} |\mathcal{N}_d^i|^2 \frac{x_W}{x_{Z_{BL}}} \\
&\quad \times (D_B - \frac{1}{2}D_{BL}) (x_{\chi_i^0}, x_{\tilde{b}_L}, x_{\tilde{b}_R}, x_{\tilde{s}_L}) \\
&\quad + \frac{\alpha_s(\mu_{EW})\alpha_{BL}m_b m_s}{24\pi\alpha_{EW}(\mu_{EW})m_W^2 c_\beta^2} \frac{(\delta^2 m_{\tilde{D}}^{LR})_{23}^* (\delta^2 m_{\tilde{D}}^{LR})_{33}}{\Lambda_{NP}^4 V_{tb} V_{ts}^*} |(U_N)_{3i}|^2 \frac{x_W}{x_{Z_{BL}}}
\end{aligned}$$

$$\begin{aligned}
& \times (D_B - \frac{1}{2}D_{BL})(x_{\chi_i^0}, x_{\tilde{b}_R}, x_{\tilde{b}_L}, x_{\tilde{s}_R}) \\
& + \frac{\alpha_s(\mu_{EW})\alpha_{BL}m_b}{24\pi\alpha_{EW}(\mu_{EW})m_Wc_Wc_\beta} \frac{(\delta^2m_{\tilde{D}}^{LL})_{23}(\delta^2m_{\tilde{D}}^{LR})_{33}}{\Lambda_{NP}^4 V_{tb}V_{ts}^*} (U_N)_{3i} \mathcal{N}_d^{i*} \frac{x_W}{x_{ZBL}} \\
& \times (D_B - \frac{1}{2}D_{BL})(x_{\chi_i^0}, x_{\tilde{b}_R}, x_{\tilde{b}_L}, x_{\tilde{s}_L}) \\
& + \frac{\alpha_s(\mu_{EW})\alpha_{BL}m_s}{24\pi\alpha_{EW}(\mu_{EW})m_Wc_Wc_\beta} \frac{(\delta^2m_{\tilde{D}}^{RR})_{23}(\delta^2m_{\tilde{D}}^{LR})_{33}^*}{\Lambda_{NP}^4 V_{tb}V_{ts}^*} (U_N)_{3i}^* \mathcal{N}_d^i \\
& \times \frac{x_W}{x_{ZBL}} (D_B - \frac{1}{2}D_{BL})(x_{\chi_i^0}, x_{\tilde{b}_L}, x_{\tilde{b}_R}, x_{\tilde{s}_R}) , \\
C_{9,\tilde{g}}^{ZBL}(\mu_{EW}) = & -\frac{\alpha_s^2(\mu_{EW})\alpha_{BL}s_W^2}{9\pi\alpha_{EW}^2(\mu_{EW})} \frac{(\delta^2m_{\tilde{D}}^{LL})_{23}}{\Lambda_{NP}^2 V_{tb}V_{ts}^*} \frac{x_W}{x_{ZBL}} (T_B - T_{BL})(x_{\tilde{g}}, x_{\tilde{b}_L}, x_{\tilde{s}_L}) \\
& + \frac{\alpha_s^2(\mu_{EW})\alpha_{BL}s_W^2}{9\pi\alpha_{EW}^2(\mu_{EW})} \frac{(\delta^2m_{\tilde{D}}^{LR})_{23}(\delta^2m_{\tilde{D}}^{LR})_{33}^*}{\Lambda_{NP}^4 V_{tb}V_{ts}^*} \frac{x_W}{x_{ZBL}} (D_B - D_{BL})(x_{\tilde{g}}, x_{\tilde{b}_L}, x_{\tilde{b}_R}, x_{\tilde{s}_L}) , \\
C_{9,\tilde{Z}BL}^{ZBL}(\mu_{EW}) = & -\frac{\alpha_s(\mu_{EW})\alpha_{BL}s_W^2}{54\pi\alpha_{EW}^2(\mu_{EW})} \frac{(\delta^2m_{\tilde{D}}^{LL})_{23}}{\Lambda_{NP}^2 V_{tb}V_{ts}^*} \frac{x_W}{x_{ZBL}} (T_B - \frac{1}{2}T_{BL})(x_{\tilde{Z}BL}, x_{\tilde{b}_L}, x_{\tilde{s}_L}) \\
& + \frac{\alpha_s(\mu_{EW})\alpha_{BL}s_W^2}{54\pi\alpha_{EW}^2(\mu_{EW})} \frac{(\delta^2m_{\tilde{D}}^{LR})_{23}(\delta^2m_{\tilde{D}}^{LR})_{33}^*}{\Lambda_{NP}^4 V_{tb}V_{ts}^*} \frac{x_W}{x_{ZBL}} (D_B - \frac{1}{2}D_{BL})(x_{\tilde{Z}BL}, x_{\tilde{b}_L}, x_{\tilde{b}_R}, x_{\tilde{s}_L}) , \\
C_{S,\tilde{Z}BL}^{H_k^0}(\mu_{EW}) = & -\frac{\alpha_{BL}m_\mu}{18\alpha_{EW}(\mu_{EW})m_W^2c_\beta^2} \frac{(\delta^2m_{\tilde{D}}^{RR})_{23}}{\Lambda_{NP}^2 V_{tb}V_{ts}^*} (Z_H)_{2k}^2 \frac{x_W}{x_{H_k^0}} T_B(x_{\tilde{Z}BL}, x_{\tilde{b}_R}, x_{\tilde{s}_R}) \\
& + \frac{\alpha_{BL}m_\mu}{18\alpha_{EW}(\mu_{EW})m_W^2c_\beta^2} \frac{(\delta^2m_{\tilde{D}}^{LR})_{23}(\delta^2m_{\tilde{D}}^{LR})_{33}^*}{\Lambda_{NP}^4 V_{tb}V_{ts}^*} (Z_H)_{2k}^2 \frac{x_W}{x_{H_k^0}} D_B(x_{\tilde{Z}BL}, x_{\tilde{b}_R}, x_{\tilde{b}_L}, x_{\tilde{s}_R}) \\
& + \frac{\alpha_{BL}m_\mu e^{i\theta_{BL}}}{9\alpha_{EW}(\mu_{EW})m_Wm_b c_W^2 c_\beta} \frac{(\delta^2m_{\tilde{D}}^{LR})_{23}}{\Lambda_{NP}^2 V_{tb}V_{ts}^*} (Z_H)_{2k} \frac{(x_W^3 x_{\tilde{Z}BL})^{1/2}}{x_{H_k^0}} \\
& \times \left[(\zeta_{LL}^s)_k \frac{\partial \varrho_{1,1}}{\partial x_{\tilde{s}_L}} + \frac{2}{3} s_W^2 (\zeta_{RR}^b)_k \frac{\partial \varrho_{1,1}}{\partial x_{\tilde{b}_R}} \right] (x_{\tilde{Z}BL}, x_{\tilde{b}_R}, x_{\tilde{s}_L}) \\
& + \frac{2\alpha_{BL}m_\mu A_{b\mu}^k e^{i\theta_{BL}}}{9\alpha_{EW}(\mu_{EW})m_W^3 c_\beta^2} \frac{(\delta^2m_{\tilde{D}}^{LL})_{23}}{\Lambda_{NP}^2 V_{tb}V_{ts}^*} (Z_H)_{2k} \frac{(x_W^3 x_{\tilde{Z}BL})^{1/2}}{x_{H_k^0}} \\
& \times \varrho_{1,1}(x_{\tilde{Z}BL}, x_{\tilde{b}_R}, x_{\tilde{b}_L}, x_{\tilde{s}_L}) \\
& - \frac{\alpha_{BL}m_\mu e^{i\theta_{BL}}}{9\alpha_{EW}(\mu_{EW})m_Wm_b c_W^2 c_\beta} \frac{(\delta^2m_{\tilde{D}}^{LL})_{23}(\delta^2m_{\tilde{D}}^{LR})_{33}}{\Lambda_{NP}^4 V_{tb}V_{ts}^*} (Z_H)_{2k} \frac{(x_W^3 x_{\tilde{Z}BL})^{1/2}}{x_{H_k^0}} \\
& \times \left[(\zeta_{LL}^s)_k \frac{\partial \varrho_{1,1}}{\partial x_{\tilde{s}_L}} + (\zeta_{LL}^b)_k \frac{\partial \varrho_{1,1}}{\partial x_{\tilde{b}_L}} + \frac{2}{3} s_W^2 (\zeta_{RR}^b)_k \frac{\partial \varrho_{1,1}}{\partial x_{\tilde{b}_R}} \right] (x_{\tilde{Z}BL}, x_{\tilde{b}_R}, x_{\tilde{b}_L}, x_{\tilde{s}_L})
\end{aligned}$$

$$\begin{aligned}
& - \frac{2\alpha_{BL} m_\mu e^{i\theta_{BL}}}{9\alpha_{EW}(\mu_{EW}) m_W^3 c_\beta^2} \frac{(\delta^2 m_{\bar{D}}^{LL})_{23} \Re[A_{b\mu}^k (\delta^2 m_{\bar{D}}^{LR})_{33}]}{\Lambda_{NP}^4 V_{tb} V_{ts}^*} (Z_H)_{2k} \frac{(x_W^3 x_{\bar{Z}_{BL}})^{1/2}}{x_{H_k^0}} \\
& \times \frac{\partial \varrho_{1,1}}{\partial x_{\bar{b}_R}} (x_{\bar{Z}_{BL}}, x_{\bar{b}_R}, x_{\bar{b}_L}, x_{\bar{s}_L}) , \\
C_{P, \bar{Z}_{BL}}^{A_k^0}(\mu_{EW}) &= \frac{\alpha_{BL} m_\mu}{18\alpha_{EW}(\mu_{EW}) m_W^2 c_\beta^2} \frac{(\delta^2 m_{\bar{D}}^{RR})_{23}}{\Lambda_{NP}^2 V_{tb} V_{ts}^*} (Z_{H^\pm})_{2k}^2 \frac{x_W}{x_{A_k^0}} T_B(x_{\bar{Z}_{BL}}, x_{\bar{b}_R}, x_{\bar{s}_R}) \\
& - \frac{\alpha_{BL} m_\mu}{18\alpha_{EW}(\mu_{EW}) m_W^2 c_\beta^2} \frac{(\delta^2 m_{\bar{D}}^{LR})_{23}^* (\delta^2 m_{\bar{D}}^{LR})_{33}}{\Lambda_{NP}^4 V_{tb} V_{ts}^*} (Z_{H^\pm})_{2k}^2 \frac{x_W}{x_{A_k^0}} D_B(x_{\bar{Z}_{BL}}, x_{\bar{b}_R}, x_{\bar{b}_L}, x_{\bar{s}_R}) \\
& - \frac{2\alpha_{BL} m_\mu P_{b\mu}^k e^{i\theta_{BL}}}{9\alpha_{EW}(\mu_{EW}) m_W^3 c_\beta^2} \frac{(\delta^2 m_{\bar{D}}^{LL})_{23}}{\Lambda_{NP}^2 V_{tb} V_{ts}^*} (Z_{H^\pm})_{2k} \frac{(x_W^3 x_{\bar{Z}_{BL}})^{1/2}}{x_{A_k^0}} \\
& \times \varrho_{1,1}(x_{\bar{Z}_{BL}}, x_{\bar{b}_R}, x_{\bar{b}_L}, x_{\bar{s}_L}) \\
& + \frac{2\alpha_{BL} m_\mu e^{i\theta_{BL}}}{9\alpha_{EW}(\mu_{EW}) m_W^3 c_\beta^2} \frac{(\delta^2 m_{\bar{D}}^{LL})_{23} \Re[P_{b\mu}^k (\delta^2 m_{\bar{D}}^{LR})_{33}]}{\Lambda_{NP}^4 V_{tb} V_{ts}^*} (Z_{H^\pm})_{2k} \frac{(x_W^3 x_{\bar{Z}_{BL}})^{1/2}}{x_{A_k^0}} \\
& \times \frac{\partial \varrho_{1,1}}{\partial x_{\bar{b}_R}} (x_{\bar{Z}_{BL}}, x_{\bar{b}_R}, x_{\bar{b}_L}, x_{\bar{s}_L}) , \\
C_{9, \bar{Z}_{BL}}^{box}(\mu_{EW}) &= - \frac{\alpha_s(\mu_{EW}) \alpha_{BL}^2 s_W^2}{36\pi \alpha_{EW}^2(\mu_{EW})} \frac{(\delta^2 m_{\bar{D}}^{LL})_{23}}{\Lambda_{NP}^2 V_{tb} V_{ts}^*} x_W \\
& \times \left[\frac{\partial \varrho_{2,1}}{\partial x_{\bar{Z}_{BL}}} - 2x_{\bar{Z}_{BL}} \frac{\partial \varrho_{1,1}}{\partial x_{\bar{Z}_{BL}}} \right] (x_{\bar{Z}_{BL}}, x_{\bar{b}_L}, x_{\bar{s}_L}, x_{\bar{e}_L}) \\
& + \frac{\alpha_s(\mu_{EW}) \alpha_{BL}^2 s_W^2}{36\pi \alpha_{EW}^2(\mu_{EW})} \frac{(\delta^2 m_{\bar{D}}^{LR})_{23} (\delta^2 m_{\bar{D}}^{LR})_{33}^*}{\Lambda_{NP}^4 V_{tb} V_{ts}^*} x_W \\
& \times \left[\frac{\partial \varrho_{2,1}}{\partial x_{\bar{Z}_{BL}}} - 2x_{\bar{Z}_{BL}} \frac{\partial \varrho_{1,1}}{\partial x_{\bar{Z}_{BL}}} \right] (x_{\bar{Z}_{BL}}, x_{\bar{b}_L}, x_{\bar{b}_R}, x_{\bar{s}_L}, x_{\bar{e}_L}) , \\
C_{9, \chi^0, \bar{Z}_{BL}}^{box}(\mu_{EW}) &= - \frac{\alpha_s(\mu_{EW}) \alpha_{BL}}{24\pi \alpha_{EW}(\mu_{EW}) c_W^2} \frac{(\delta^2 m_{\bar{D}}^{LL})_{23}}{\Lambda_{NP}^2 V_{tb} V_{ts}^*} x_W \left[\Re(\mathcal{N}_d^{i*} \mathcal{N}_l^i) \varrho_{2,1} \right. \\
& - \frac{4s_W}{c_W} \Re(e^{i\theta_{BL}} (U_N)_{1i} \mathcal{N}_d^i) (x_{\chi_i^0} x_{\bar{Z}_{BL}})^{1/2} \varrho_{1,1} \left. \right] (x_{\chi_i^0}, x_{\bar{Z}_{BL}}, x_{\bar{b}_L}, x_{\bar{s}_L}, x_{\bar{e}_L}) \\
& - \frac{\alpha_s(\mu_{EW}) \alpha_{BL} m_\mu m_s}{48\pi \alpha_{EW}(\mu_{EW}) m_W^2 c_\beta^2} \frac{(\delta^2 m_{\bar{D}}^{RR})_{23}}{\Lambda_{NP}^2 V_{tb} V_{ts}^*} (U_N)_{3i}^* (U_N)_{3i} x_W \\
& \times \varrho_{2,1}(x_{\chi_i^0}, x_{\bar{Z}_{BL}}, x_{\bar{b}_R}, x_{\bar{s}_R}, x_{\bar{e}_R}) \\
& - \frac{\alpha_s(\mu_{EW}) \alpha_{BL}}{48\pi \alpha_{EW}(\mu_{EW})} \frac{(\delta^2 m_{\bar{D}}^{LR})_{23}}{\Lambda_{NP}^2 V_{tb} V_{ts}^*} x_W \left[\frac{m_b}{m_W c_W c_\beta} \mathcal{N}_l^{i*}(U_N)_{3i} \varrho_{2,1} + \frac{m_\mu}{m_W c_\beta} \mathcal{N}_d^{i*}(U_N)_{3i} \varrho_{2,1} \right.
\end{aligned}$$

$$\begin{aligned}
& -\frac{4m_b s_W e^{i\theta_{BL}}}{m_W c_\beta} (U_N)_{1i} (U_N)_{3i} (x_{\chi_i^0} x_{\tilde{Z}_{BL}})^{1/2} \varrho_{1,1} \Big] (x_{\chi_i^0}, x_{\tilde{Z}_{BL}}, x_{\tilde{b}_R}, x_{\tilde{s}_L}, x_{\tilde{e}_L}) \\
& -\frac{\alpha_s(\mu_{EW})\alpha_{BL}}{24\pi\alpha_{EW}(\mu_{EW})m_W c_W^2 c_\beta} \frac{(\delta^2 m_{\tilde{D}}^{LR})_{23}^*}{\Lambda_{NP}^2 V_{tb} V_{ts}^*} x_W \Big[(U_N)_{3i}^* \mathcal{N}_l^i \varrho_{2,1} \\
& -4s_W e^{i\theta_{BL}} (U_N)_{3i}^* (U_N)_{1i}^* (x_{\chi_i^0} x_{\tilde{Z}_{BL}})^{1/2} \varrho_{1,1} \Big] (x_{\chi_i^0}, x_{\tilde{Z}_{BL}}, x_{\tilde{b}_L}, x_{\tilde{s}_R}, x_{\tilde{e}_R}) \\
& +\frac{\alpha_s(\mu_{EW})\alpha_{BL}}{24\pi\alpha_{EW}(\mu_{EW})c_W^2} \frac{(\delta^2 m_{\tilde{D}}^{LR})_{23} (\delta^2 m_{\tilde{D}}^{LR})_{33}^*}{\Lambda_{NP}^4 V_{tb} V_{ts}^*} x_W \Big[\Re(e^{i\theta_{BL}} \mathcal{N}_d^{i*} \mathcal{N}_l^i) \varrho_{2,1} \\
& -\frac{4s_W}{c_W} \Re((U_N)_{1i} \mathcal{N}_d^i) (x_{\chi_i^0} x_{\tilde{Z}_{BL}})^{1/2} \varrho_{1,1} \Big] (x_{\chi_i^0}, x_{\tilde{Z}_{BL}}, x_{\tilde{b}_L}, x_{\tilde{b}_R}, x_{\tilde{s}_L}, x_{\tilde{e}_L}) \\
& +\frac{\alpha_s(\mu_{EW})\alpha_{BL} m_\mu m_s}{48\pi\alpha_{EW}(\mu_{EW})m_W^2 c_\beta^2} \frac{(\delta^2 m_{\tilde{D}}^{LR})_{23}^* (\delta^2 m_{\tilde{D}}^{LR})_{33}}{\Lambda_{NP}^4 V_{tb} V_{ts}^*} (U_N)_{3i}^* (U_N)_{3i} x_W \\
& \times \varrho_{2,1} (x_{\chi_i^0}, x_{\tilde{Z}_{BL}}, x_{\tilde{b}_R}, x_{\tilde{b}_L}, x_{\tilde{s}_R}, x_{\tilde{e}_R}) \\
& +\frac{\alpha_s(\mu_{EW})\alpha_{BL}}{48\pi\alpha_{EW}(\mu_{EW})} \frac{(\delta^2 m_{\tilde{D}}^{LL})_{23} (\delta^2 m_{\tilde{D}}^{LR})_{33}}{\Lambda_{NP}^4 V_{tb} V_{ts}^*} x_W \Big[\frac{m_b}{m_W c_W c_\beta} \mathcal{N}_l^{i*} (U_N)_{3i} \varrho_{2,1} \\
& +\frac{m_\mu}{m_W c_\beta} \mathcal{N}_d^{i*} (U_N)_{3i} \varrho_{2,1} \\
& -\frac{4m_b s_W}{m_W c_\beta} e^{i\theta_{BL}} (U_N)_{1i} (U_N)_{3i} (x_{\chi_i^0} x_{\tilde{Z}_{BL}})^{1/2} \varrho_{1,1} \Big] (x_{\chi_i^0}, x_{\tilde{Z}_{BL}}, x_{\tilde{b}_R}, x_{\tilde{b}_L}, x_{\tilde{s}_L}, x_{\tilde{e}_L}) \\
& +\frac{\alpha_s(\mu_{EW})\alpha_{BL}}{24\pi\alpha_{EW}(\mu_{EW})m_W c_W^2 c_\beta} \frac{(\delta^2 m_{\tilde{D}}^{RR})_{23} (\delta^2 m_{\tilde{D}}^{LR})_{33}^*}{\Lambda_{NP}^4 V_{tb} V_{ts}^*} x_W \Big[(U_N)_{3i}^* \mathcal{N}_l^i \varrho_{2,1} \\
& -4s_W e^{i\theta_{BL}} (U_N)_{3i}^* (U_N)_{1i}^* (x_{\chi_i^0} x_{\tilde{Z}_{BL}})^{1/2} \varrho_{1,1} \Big] (x_{\chi_i^0}, x_{\tilde{Z}_{BL}}, x_{\tilde{b}_L}, x_{\tilde{b}_R}, x_{\tilde{s}_R}, x_{\tilde{e}_R}) , \\
C_{10, \tilde{Z}_{BL}}^{box}(\mu_{EW}) &= \frac{\alpha_s(\mu_{EW})\alpha_{BL}^2 s_W^2}{36\pi\alpha_{EW}^2(\mu_{EW})} \frac{(\delta^2 m_{\tilde{D}}^{LL})_{23}}{\Lambda_{NP}^2 V_{tb} V_{ts}^*} x_W \\
& \times \Big[\frac{\partial \varrho_{2,1}}{\partial x_{\tilde{Z}_{BL}}} + 2x_{\tilde{Z}_{BL}} \frac{\partial \varrho_{1,1}}{\partial x_{\tilde{Z}_{BL}}} \Big] (x_{\tilde{Z}_{BL}}, x_{\tilde{b}_L}, x_{\tilde{s}_L}, x_{\tilde{e}_L}) \\
& -\frac{\alpha_s(\mu_{EW})\alpha_{BL}^2 s_W^2}{36\pi\alpha_{EW}^2(\mu_{EW})} \frac{(\delta^2 m_{\tilde{D}}^{LR})_{23} (\delta^2 m_{\tilde{D}}^{LR})_{33}^*}{\Lambda_{NP}^4 V_{tb} V_{ts}^*} x_W \\
& \times \Big[\frac{\partial \varrho_{2,1}}{\partial x_{\tilde{Z}_{BL}}} + 2x_{\tilde{Z}_{BL}} \frac{\partial \varrho_{1,1}}{\partial x_{\tilde{Z}_{BL}}} \Big] (x_{\tilde{Z}_{BL}}, x_{\tilde{b}_L}, x_{\tilde{b}_R}, x_{\tilde{s}_L}, x_{\tilde{e}_L}) , \\
C_{10, \chi^0 \tilde{Z}_{BL}}^{box}(\mu_{EW}) &= \frac{\alpha_s(\mu_{EW})\alpha_{BL}}{24\pi\alpha_{EW}(\mu_{EW})c_W^2} \frac{(\delta^2 m_{\tilde{D}}^{LL})_{23}}{\Lambda_{NP}^2 V_{tb} V_{ts}^*} x_W \Big[\Re(\mathcal{N}_d^{i*} \mathcal{N}_l^i) \varrho_{2,1} \\
& +\frac{4s_W}{c_W} \Re(e^{i\theta_{BL}} (U_N)_{1i} \mathcal{N}_d^i) (x_{\chi_i^0} x_{\tilde{Z}_{BL}})^{1/2} \varrho_{1,1} \Big] (x_{\chi_i^0}, x_{\tilde{Z}_{BL}}, x_{\tilde{b}_L}, x_{\tilde{s}_L}, x_{\tilde{e}_L}) \\
& +\frac{\alpha_s(\mu_{EW})\alpha_{BL} m_\mu m_s}{48\pi\alpha_{EW}(\mu_{EW})m_W^2 c_\beta^2} \frac{(\delta^2 m_{\tilde{D}}^{RR})_{23}}{\Lambda_{NP}^2 V_{tb} V_{ts}^*} (U_N)_{3i}^* (U_N)_{3i} x_W
\end{aligned}$$

$$\begin{aligned}
& \times \varrho_{2,1}(x_{\chi_i^0}, x_{\tilde{Z}_{BL}}, x_{\tilde{b}_R}, x_{\tilde{s}_R}, x_{\tilde{e}_R}) \\
& + \frac{\alpha_s(\mu_{EW})\alpha_{BL}}{48\pi\alpha_{EW}(\mu_{EW})} \frac{(\delta^2 m_{\tilde{D}}^{LR})_{23}}{\Lambda_{NP}^2 V_{tb} V_{ts}^*} x_W \left[\frac{m_b}{m_W c_W c_\beta} \mathcal{N}_l^{i*}(U_N)_{3i} \varrho_{2,1} + \frac{m_\mu}{m_W c_\beta} \mathcal{N}_d^{i*}(U_N)_{3i} \varrho_{2,1} \right. \\
& + \left. \frac{4m_b s_W}{m_W c_\beta} e^{i\theta_{BL}} (U_N)_{1i} (U_N)_{3i} (x_{\chi_i^0} x_{\tilde{Z}_{BL}})^{1/2} \varrho_{1,1} \right] (x_{\chi_i^0}, x_{\tilde{Z}_{BL}}, x_{\tilde{b}_R}, x_{\tilde{s}_L}, x_{\tilde{e}_L}) \\
& + \frac{\alpha_s(\mu_{EW})\alpha_{BL}}{24\pi\alpha_{EW}(\mu_{EW}) m_W c_W^2 c_\beta} \frac{(\delta^2 m_{\tilde{D}}^{LR})_{23}^*}{\Lambda_{NP}^2 V_{tb} V_{ts}^*} x_W \left[(U_N)_{3i}^* \mathcal{N}_l^i \varrho_{2,1} \right. \\
& + \left. 4s_W e^{i\theta_{BL}} (U_N)_{3i}^* (U_N)_{1i}^* (x_{\chi_i^0} x_{\tilde{Z}_{BL}})^{1/2} \varrho_{1,1} \right] (x_{\chi_i^0}, x_{\tilde{Z}_{BL}}, x_{\tilde{b}_L}, x_{\tilde{s}_R}, x_{\tilde{e}_R}) \\
& - \frac{\alpha_s(\mu_{EW})\alpha_{BL}}{24\pi\alpha_{EW}(\mu_{EW}) c_W^2} \frac{(\delta^2 m_{\tilde{D}}^{LR})_{23} (\delta^2 m_{\tilde{D}}^{LR})_{33}^*}{\Lambda_{NP}^4 V_{tb} V_{ts}^*} x_W \left[\Re(\mathcal{N}_d^{i*} \mathcal{N}_l^i) \varrho_{2,1} \right. \\
& + \left. \frac{4s_W}{c_W} \Re(e^{i\theta_{BL}} (U_N)_{1i} \mathcal{N}_d^i) (x_{\chi_i^0} x_{\tilde{Z}_{BL}})^{1/2} \varrho_{1,1} \right] (x_{\chi_i^0}, x_{\tilde{Z}_{BL}}, x_{\tilde{b}_L}, x_{\tilde{b}_R}, x_{\tilde{s}_L}, x_{\tilde{e}_L}) \\
& - \frac{\alpha_s(\mu_{EW})\alpha_{BL} m_\mu m_s}{48\pi\alpha_{EW}(\mu_{EW}) m_W^2 c_\beta^2} \frac{(\delta^2 m_{\tilde{D}}^{LR})_{23}^* (\delta^2 m_{\tilde{D}}^{LR})_{33}}{\Lambda_{NP}^4 V_{tb} V_{ts}^*} (U_N)_{3i}^* (U_N)_{3i} x_W \\
& \times \varrho_{2,1}(x_{\chi_i^0}, x_{\tilde{Z}_{BL}}, x_{\tilde{b}_R}, x_{\tilde{b}_L}, x_{\tilde{s}_R}, x_{\tilde{e}_R}) \\
& - \frac{\alpha_s(\mu_{EW})\alpha_{BL}}{48\pi\alpha_{EW}(\mu_{EW})} \frac{(\delta^2 m_{\tilde{D}}^{LL})_{23} (\delta^2 m_{\tilde{D}}^{LR})_{33}}{\Lambda_{NP}^4 V_{tb} V_{ts}^*} x_W \left[\frac{m_b}{m_W c_W c_\beta} \mathcal{N}_l^{i*}(U_N)_{3i} \varrho_{2,1} \right. \\
& + \frac{m_\mu}{m_W c_\beta} \mathcal{N}_d^{i*}(U_N)_{3i} \varrho_{2,1} \\
& + \left. \frac{4m_b s_W}{m_W c_\beta} e^{i\theta_{BL}} (U_N)_{1i} (U_N)_{3i} (x_{\chi_i^0} x_{\tilde{Z}_{BL}})^{1/2} \varrho_{1,1} \right] (x_{\chi_i^0}, x_{\tilde{Z}_{BL}}, x_{\tilde{b}_R}, x_{\tilde{b}_L}, x_{\tilde{s}_L}, x_{\tilde{e}_L}) \\
& - \frac{\alpha_s(\mu_{EW})\alpha_{BL}}{24\pi\alpha_{EW}(\mu_{EW}) m_W c_W^2 c_\beta} \frac{(\delta^2 m_{\tilde{D}}^{RR})_{23} (\delta^2 m_{\tilde{D}}^{LR})_{33}^*}{\Lambda_{NP}^4 V_{tb} V_{ts}^*} x_W \left[(U_N)_{3i}^* \mathcal{N}_l^i \varrho_{2,1} \right. \\
& + \left. 4s_W e^{i\theta_{BL}} (U_N)_{3i}^* (U_N)_{1i}^* (x_{\chi_i^0} x_{\tilde{Z}_{BL}})^{1/2} \varrho_{1,1} \right] (x_{\chi_i^0}, x_{\tilde{Z}_{BL}}, x_{\tilde{b}_L}, x_{\tilde{b}_R}, x_{\tilde{s}_R}, x_{\tilde{e}_R}), \\
C_{S, \chi^0 \tilde{Z}_{BL}}^{box}(\mu_{EW}) = & - \frac{\alpha_{BL} m_\mu}{6\alpha_{EW}(\mu_{EW}) m_W^2 c_\beta^2} \frac{(\delta^2 m_{\tilde{D}}^{LL})_{23}}{\Lambda_{NP}^2 V_{tb} V_{ts}^*} x_W \left[(U_N)_{3i} (U_N)_{3i}^* \varrho_{2,1} \right. \\
& - \frac{e^{i\theta_{BL}}}{c_W} (U_N)_{3i}^* (U_N)_{3i} (x_{\chi_i^0} x_{\tilde{Z}_{BL}})^{1/2} \varrho_{1,1} \left. \right] (x_{\chi_i^0}, x_{\tilde{Z}_{BL}}, x_{\tilde{b}_L}, x_{\tilde{s}_L}, x_{\tilde{e}_L}) \\
& - \frac{\alpha_{BL} m_\mu m_s e^{i\theta_{BL}}}{6\alpha_{EW}(\mu_{EW}) m_W^2 m_b c_\beta^2} \frac{(\delta^2 m_{\tilde{D}}^{RR})_{23}}{\Lambda_{NP}^2 V_{tb} V_{ts}^*} x_W (U_N)_{3i}^* (U_N)_{3i} (x_{\chi_i^0} x_{\tilde{Z}_{BL}})^{1/2} \\
& \times \varrho_{1,1}(x_{\chi_i^0}, x_{\tilde{Z}_{BL}}, x_{\tilde{b}_R}, x_{\tilde{s}_R}, x_{\tilde{e}_L}) \\
& - \frac{\alpha_{BL} m_\mu}{18\alpha_{EW}(\mu_{EW}) m_W m_b c_W c_\beta} \frac{(\delta^2 m_{\tilde{D}}^{LR})_{23}}{\Lambda_{NP}^2 V_{tb} V_{ts}^*} x_W \left[2s_W (U_N)_{3i} (U_N)_{1i}^* \varrho_{2,1} \right. \\
& + \left. 3c_W e^{i\theta_{BL}} \mathcal{N}_d^{i*}(U_N)_{3i} (x_{\chi_i^0} x_{\tilde{Z}_{BL}})^{1/2} \varrho_{1,1} \right]
\end{aligned}$$

$$\begin{aligned}
& -2s_W e^{i\theta_{BL}} (U_N)^*_{3i} (U_N)^*_{1i} (x_{\chi_i^0} x_{\tilde{Z}_{BL}})^{1/2} \varrho_{1,1} \Big] (x_{\chi_i^0}, x_{\tilde{Z}_{BL}}, x_{\tilde{b}_R}, x_{\tilde{s}_L}, x_{\tilde{e}_R}) \\
& + \frac{\alpha_{BL} m_\mu}{6\alpha_{EW} (\mu_{EW}) m_W^2 c_\beta^2} \frac{(\delta^2 m_{\tilde{D}}^{LR})_{23} (\delta^2 m_{\tilde{D}}^{LR})_{33}^*}{\Lambda_{NP}^4 V_{tb} V_{ts}^*} x_W \Big[(U_N)_{3i} (U_N)^*_{3i} \varrho_{2,1} \\
& - \frac{e^{i\theta_{BL}}}{c_W} (U_N)^*_{3i} (U_N)^*_{3i} (x_{\chi_i^0} x_{\tilde{Z}_{BL}})^{1/2} \varrho_{1,1} \Big] (x_{\chi_i^0}, x_{\tilde{Z}_{BL}}, x_{\tilde{b}_L}, x_{\tilde{b}_R}, x_{\tilde{s}_L}, x_{\tilde{e}_L}) \\
& + \frac{\alpha_{BL} m_\mu m_s e^{i\theta_{BL}}}{6\alpha_{EW} (\mu_{EW}) m_W^2 m_b c_\beta^2} \frac{(\delta^2 m_{\tilde{D}}^{LR})_{23}^* (\delta^2 m_{\tilde{D}}^{LR})_{33}}{\Lambda_{NP}^4 V_{tb} V_{ts}^*} x_W (U_N)^*_{3i} (U_N)^*_{3i} (x_{\chi_i^0} x_{\tilde{Z}_{BL}})^{1/2} \\
& \times \varrho_{1,1} (x_{\chi_i^0}, x_{\tilde{Z}_{BL}}, x_{\tilde{b}_R}, x_{\tilde{b}_L}, x_{\tilde{s}_R}, x_{\tilde{e}_L}) \\
& + \frac{\alpha_{BL} m_\mu}{18\alpha_{EW} (\mu_{EW}) m_W m_b c_W c_\beta} \frac{(\delta^2 m_{\tilde{D}}^{LL})_{23} (\delta^2 m_{\tilde{D}}^{LR})_{33}}{\Lambda_{NP}^4 V_{tb} V_{ts}^*} x_W \\
& \times \Big[2s_W (U_N)_{3i} (U_N)^*_{1i} \varrho_{2,1} + 3c_W e^{i\theta_{BL}} \mathcal{N}_d^{i*} (U_N)^*_{3i} (x_{\chi_i^0} x_{\tilde{Z}_{BL}})^{1/2} \varrho_{1,1} \\
& - 2s_W e^{i\theta_{BL}} (U_N)^*_{3i} (U_N)^*_{1i} (x_{\chi_i^0} x_{\tilde{Z}_{BL}})^{1/2} \varrho_{1,1} \Big] (x_{\chi_i^0}, x_{\tilde{Z}_{BL}}, x_{\tilde{b}_R}, x_{\tilde{b}_L}, x_{\tilde{s}_L}, x_{\tilde{e}_R}), \\
C_{P, \chi^0 \tilde{Z}_{BL}}^{box} (\mu_{EW}) &= \frac{\alpha_{BL} m_\mu}{6\alpha_{EW} (\mu_{EW}) m_W^2 c_\beta^2} \frac{(\delta^2 m_{\tilde{D}}^{LL})_{23}}{\Lambda_{NP}^2 V_{tb} V_{ts}^*} x_W \Big[(U_N)_{3i} (U_N)^*_{3i} \varrho_{2,1} \\
& + \frac{e^{i\theta_{BL}}}{c_W} (U_N)^*_{3i} (U_N)^*_{3i} (x_{\chi_i^0} x_{\tilde{Z}_{BL}})^{1/2} \varrho_{1,1} \Big] (x_{\chi_i^0}, x_{\tilde{Z}_{BL}}, x_{\tilde{b}_L}, x_{\tilde{s}_L}, x_{\tilde{e}_L}) \\
& - \frac{\alpha_{BL} m_\mu m_s e^{i\theta_{BL}}}{6\alpha_{EW} (\mu_{EW}) m_W^2 m_b c_\beta^2} \frac{(\delta^2 m_{\tilde{D}}^{RR})_{23}}{\Lambda_{NP}^2 V_{tb} V_{ts}^*} (U_N)^*_{3i} (U_N)^*_{3i} x_W (x_{\chi_i^0} x_{\tilde{Z}_{BL}})^{1/2} \\
& \times \varrho_{1,1} (x_{\chi_i^0}, x_{\tilde{Z}_{BL}}, x_{\tilde{b}_R}, x_{\tilde{s}_R}, x_{\tilde{e}_L}) \\
& + \frac{\alpha_{BL} m_\mu}{18\alpha_{EW} (\mu_{EW}) m_W m_b c_W c_\beta} \frac{(\delta^2 m_{\tilde{D}}^{LR})_{23}}{\Lambda_{NP}^2 V_{tb} V_{ts}^*} x_W \\
& \times \Big[2s_W (U_N)_{3i} (U_N)^*_{1i} \varrho_{2,1} - 3c_W e^{i\theta_{BL}} \mathcal{N}_d^{i*} (U_N)^*_{3i} (x_{\chi_i^0} x_{\tilde{Z}_{BL}})^{1/2} \varrho_{1,1} \\
& + 2s_W e^{i\theta_{BL}} (U_N)^*_{3i} (U_N)^*_{1i} (x_{\chi_i^0} x_{\tilde{Z}_{BL}})^{1/2} \varrho_{1,1} \Big] (x_{\chi_i^0}, x_{\tilde{Z}_{BL}}, x_{\tilde{b}_R}, x_{\tilde{s}_L}, x_{\tilde{e}_R}) \\
& - \frac{\alpha_{BL} m_\mu}{6\alpha_{EW} (\mu_{EW}) m_W^2 c_\beta^2} \frac{(\delta^2 m_{\tilde{D}}^{LR})_{23} (\delta^2 m_{\tilde{D}}^{LR})_{33}^*}{\Lambda_{NP}^4 V_{tb} V_{ts}^*} x_W \Big[(U_N)_{3i} (U_N)^*_{3i} \varrho_{2,1} \\
& + \frac{e^{i\theta_{BL}}}{c_W} (U_N)^*_{3i} (U_N)^*_{3i} (x_{\chi_i^0} x_{\tilde{Z}_{BL}})^{1/2} \varrho_{1,1} \Big] (x_{\chi_i^0}, x_{\tilde{Z}_{BL}}, x_{\tilde{b}_L}, x_{\tilde{b}_R}, x_{\tilde{s}_L}, x_{\tilde{e}_L}) \\
& + \frac{\alpha_{BL} m_\mu m_s e^{i\theta_{BL}}}{6\alpha_{EW} (\mu_{EW}) m_W^2 m_b c_\beta^2} \frac{(\delta^2 m_{\tilde{D}}^{LR})_{23}^* (\delta^2 m_{\tilde{D}}^{LR})_{33}}{\Lambda_{NP}^4 V_{tb} V_{ts}^*} (U_N)^*_{3i} (U_N)^*_{3i} x_W (x_{\chi_i^0} x_{\tilde{Z}_{BL}})^{1/2} \\
& \times \varrho_{1,1} (x_{\chi_i^0}, x_{\tilde{Z}_{BL}}, x_{\tilde{b}_R}, x_{\tilde{b}_L}, x_{\tilde{s}_R}, x_{\tilde{e}_L}) \\
& - \frac{\alpha_{BL} m_\mu}{18\alpha_{EW} (\mu_{EW}) m_W m_b c_W c_\beta} \frac{(\delta^2 m_{\tilde{D}}^{LL})_{23} (\delta^2 m_{\tilde{D}}^{LR})_{33}}{\Lambda_{NP}^4 V_{tb} V_{ts}^*} x_W
\end{aligned}$$

$$\begin{aligned}
& \times \left[2s_W(U_N)_{3i}(U_N)_{1i}^* \varrho_{2,1} - 3c_W e^{i\theta_{BL}} \mathcal{N}_d^{i*} (U_N)_{3i}^* (x_{\chi_i^0} x_{\tilde{Z}_{BL}})^{1/2} \varrho_{1,1} \right. \\
& \left. + 2s_W e^{i\theta_{BL}} (U_N)_{3i}^* (U_N)_{1i}^* (x_{\chi_i^0} x_{\tilde{Z}_{BL}})^{1/2} \varrho_{1,1} \right] (x_{\chi_i^0}, x_{\tilde{Z}_{BL}}, x_{\tilde{b}_R}, x_{\tilde{b}_L}, x_{\tilde{s}_L}, x_{\tilde{e}_R}) , \quad (B1)
\end{aligned}$$

where the couplings in the expression are

$$\begin{aligned}
\mathcal{N}_d^i &= \frac{1}{3} (U_N)_{1i} s_W - (U_N)_{2i} c_W , \\
\mathcal{N}_l^i &= (U_N)_{1i} s_W + (U_N)_{2i} c_W , \\
\mathcal{C}_{ij}^L &= 2(c_W^2 - s_W^2) \delta_{ij} + (U_-)_{1i}^* (U_-)_{1j} , \\
\mathcal{C}_{ij}^R &= 2(c_W^2 - s_W^2) \delta_{ij} + (U_+)_{1i} (U_+)_{1j}^* , \\
B_H^k &= \cos \beta (Z_H)_{1k} - \sin \beta (Z_H)_{2k} , \\
(\zeta_{LL}^u)_k &= (1 - \frac{4}{3} s_W^2) B_H^k + \frac{2m_u^2 c_W^2}{m_W^2 s_\beta} (Z_H)_{1k} , \\
(\zeta_{RR}^u)_k &= B_H^k + \frac{3m_u^2 c_W^2}{2m_W^2 s_W^2 s_\beta} (Z_H)_{1k} , \\
(\zeta_{LL}^d)_k &= (1 - \frac{2}{3} s_W^2) B_H^k - \frac{2m_d^2 c_W^2}{m_W^2 c_\beta} (Z_H)_{2k} , \\
(\zeta_{RR}^d)_k &= B_H^k - \frac{3m_d^2 c_W^2}{m_W^2 s_W^2 c_\beta} (Z_H)_{2k} , \\
(\xi_k^{\chi^\pm})_{ij} &= (Z_H)_{1k} (U_-)_{1i} (U_+)_{2j} + (Z_H)_{2k} (U_-)_{2i} (U_+)_{1j} , \\
(\xi_k^{\chi^0})_{ij} &= [(Z_H)_{1k} (U_N)_{3j} - (Z_H)_{2k} (U_N)_{4j}] [(U_N)_{1i} s_W - (U_N)_{2i} c_W] , \\
(\eta_k^{\chi^\pm})_{ij} &= (Z_{H^\pm})_{1k} (U_-)_{1i} (U_+)_{2j} + (Z_{H^\pm})_{2k} (U_-)_{2i} (U_+)_{1j} , \\
(\eta_k^{\chi^0})_{ij} &= [(Z_{H^\pm})_{1k} (U_N)_{3j} - (Z_{H^\pm})_{2k} (U_N)_{4j}] [(U_N)_{1i} s_W - (U_N)_{2i} c_W] , \\
A_M^{ki} &= (Z_H)_{1k} (Z_{H^\pm})_{1i} - (Z_H)_{2k} (Z_{H^\pm})_{2i} , \\
A_{u\mu}^k &= A_u (Z_H)_{1k} + \mu^* (Z_H)_{2k} , \\
A_{d\mu}^k &= A_d (Z_H)_{2k} + \mu^* (Z_H)_{1k} , \\
P_{u\mu}^k &= A_u (Z_{H^\pm})_{1k} - \mu^* (Z_{H^\pm})_{2k} , \\
P_{d\mu}^k &= A_d (Z_{H^\pm})_{2k} - \mu^* (Z_{H^\pm})_{1k} . \quad (B2)
\end{aligned}$$

Here U_N , U_\pm are the mixing matrices of neutralinos and charginos in the MSSM, respectively. Z_H is the 2×2 mixing matrix of CP-even Higgs, and

$$Z_{H^\pm} = \begin{pmatrix} c_\beta & -s_\beta \\ s_\beta & c_\beta \end{pmatrix} \quad (\text{B3})$$

is the mixing matrix between charged Higgs and Goldstone. Furthermore, we adopt the shorten-cutting notations as $c_\beta = \cos \beta$, $s_\beta = \sin \beta$, $c_W = \cos \theta_W$, $s_W = \sin \theta_W$.

Appendix C: The functions

The functions in the wilson coefficients of γ - and g - penguin operators are

$$\begin{aligned} T_B(x, y, z) &= \left[2\varrho_{1,1} - \frac{\partial \varrho_{2,1}}{\partial x} \right] (x, y, z) , \\ T_{BL}(x, y, z) &= \frac{\partial \varrho_{2,1}}{\partial y} + \frac{\partial \varrho_{2,1}}{\partial z} , \\ T_1(x, y, z) &= \left[\frac{\partial \varrho_{1,1}}{\partial y} + \frac{\partial \varrho_{1,1}}{\partial z} \right] (x, y, z) , \\ T_2(x, y, z) &= \left[\frac{\partial^2 \varrho_{2,1}}{\partial y^2} + 2 \frac{\partial^2 \varrho_{2,1}}{\partial y \partial z} + \frac{\partial^2 \varrho_{2,1}}{\partial z^2} \right] (x, y, z) , \\ T_3(x, y, z) &= \left[\frac{\partial^3 \varrho_{3,1}}{\partial y^3} + 3 \frac{\partial^3 \varrho_{3,1}}{\partial y^2 \partial z} + 3 \frac{\partial^3 \varrho_{3,1}}{\partial y \partial z^2} + \frac{\partial^3 \varrho_{3,1}}{\partial z^3} \right] (x, y, z) , \end{aligned} \quad (\text{C1})$$

and

$$\begin{aligned} D_B(x, y, z, u) &= \left[2\varrho_{1,1} - \frac{\partial \varrho_{2,1}}{\partial x} \right] (x, y, z, u) , \\ D_{BL}(x, y, z, u) &= \frac{\partial \varrho_{2,1}}{\partial y} + \frac{\partial \varrho_{2,1}}{\partial z} + \frac{\partial \varrho_{2,1}}{\partial u} , \\ D_1(x, y, z, u) &= \left[\frac{\partial \varrho_{1,1}}{\partial y} + \frac{\partial \varrho_{1,1}}{\partial z} + \frac{\partial \varrho_{1,1}}{\partial u} \right] (x, y, z, u) , \\ D_2(x, y, z, u) &= \left[\frac{\partial^2 \varrho_{2,1}}{\partial y^2} + 2 \frac{\partial^2 \varrho_{2,1}}{\partial y \partial z} + 2 \frac{\partial^2 \varrho_{2,1}}{\partial y \partial u} + \frac{\partial^2 \varrho_{2,1}}{\partial z^2} + 2 \frac{\partial^2 \varrho_{2,1}}{\partial z \partial u} + \frac{\partial^2 \varrho_{2,1}}{\partial u^2} \right] (x, y, z, u) , \\ D_3(x, y, z, u) &= \left[\frac{\partial^3 \varrho_{3,1}}{\partial y^3} + 3 \frac{\partial^3 \varrho_{3,1}}{\partial y^2 \partial z} + 3 \frac{\partial^3 \varrho_{3,1}}{\partial y^2 \partial u} + 3 \frac{\partial^3 \varrho_{3,1}}{\partial y \partial z^2} + 6 \frac{\partial^3 \varrho_{3,1}}{\partial y \partial z \partial u} + 3 \frac{\partial^3 \varrho_{3,1}}{\partial y \partial u^2} \right. \\ &\quad \left. + \frac{\partial^3 \varrho_{3,1}}{\partial z^3} + 3 \frac{\partial^3 \varrho_{3,1}}{\partial z^2 \partial u} + 3 \frac{\partial^3 \varrho_{3,1}}{\partial z \partial u^2} + \frac{\partial^3 \varrho_{3,1}}{\partial u^3} \right] (x, y, z, u) \end{aligned} \quad (\text{C2})$$

with

$$\varrho_{m,n}(x_1, x_2, \dots, x_N) = \sum_{i=1}^N \frac{x_i^m \ln^n x_i}{\prod_{j \neq i}^N (x_i - x_j)} . \quad (\text{C3})$$

- [1] G. Buchalla, A. J. Buras, Nucl. Phys. B**400**(1993)225.
- [2] M. Misiak, Nucl. Phys. B**393**(1993)23[Erratum-ibid. B**439**(1995)461].
- [3] A. J. Buras, M. Münz, Phys. Rev. D**52**(1995)186.
- [4] G. Buchalla, A. J. Buras, M. E. Lautenbacher, Rev. Mod. Phys. **68**(1996)1125.
- [5] N. G. Deshpande, J. Trampetic, K. Panose, Phys. Rev. D**39**(1989)1461.
- [6] C. S. Lim, T. Morozumi, A. I. Sanda, Phys. Lett. B**218**(1989)343.
- [7] P. J. O'Donnell, H.K.K. Tung, Phys. Rev. D**43**(1991)2067.
- [8] A. Buras, M. Misiak and J. Urban, Nucl. Phys. B**586**(2000)397;
- [9] C. Bobeth, M. Misiak and J. Urban, Nucl. Phys. B**574**(2000)291; H. H. Asatrian, H. M. Asatrian, C. Greub and M. Walker, Phys. Lett. B**507**(2001)162, Phys. Rev. D**65**(2002)074004; C. Bother, P. Gambino, M. Gorbahn and U. Haisch, JHEP0404(2004)071; A. Ghinculov, T. Hurth, G. Isidori and Y. Yao, Nucl. Phys. B**685**(2004)351; Z. Ligeti, F. J. Tackmann, Phys. Lett. B**653**(2007)404; C. Greub, V. Pilipp and C. Schupbach, JHEP0812(2008)040.
- [10] T. Hurth, G. Isidori, J. F. Kamenik and F. Mescia, Nucl. Phys. B**808**(2009)326.
- [11] T. Huber, E. Lunghi, M. Misiak and D. Wyler, Nucl. Phys. B**740**(2006)105.
- [12] B. Aubert *et al.*, BABAR collaboration, Phys. Rev. Lett.**93**(2004)081802; J. Lees *et al.*, BABAR collaboration, Phys. Rev. D**86**(2012)032012.
- [13] M. Iwasaki *et al.*, BELLE collaboration, Phys. Rev. D**72**(2005)092005; J. Wei *et al.*, BELLE collaboration, Phys. Rev. Lett.**103**(2009)171801.
- [14] D. Asner *et al.*, Heavy Flavor Average Group collaboration, *Averages of B-hadron, c-hadron and τ -lepton properties*, arXiv:1010.1589.
- [15] Y. Sato *et al.*, BELLE collaboration, Phys. Rev. D**93**(2016)032008; *ibid.***93**(2016)059901.
- [16] S. Fukae, C. S. Kim, T. Morozumi and T. Yoshikawa, Phys. Rev. D**59**(1999)074013; A. Ali, E. Lunghi, C. Greub, and G. Hiller, Phys. Rev. D**66**(2002)034002.

- [17] A. Ali, G. Hiller, Eur. Phys. J. C **8**(1999)619.
- [18] A. Soni, A.K. Alok, A. Giri, R. Mohanta, S. Nandi, Phys. Rev. D **82**(2010)033009; A. K. Alok, A. Dighe and S.Ray, Phys. Rev. D **79**(2009)034017.
- [19] J. Lees *et al.*, BABAR collaboration, Phys. Rev. Lett. **112**(2014)211802.
- [20] E. Gabrielli *et al.*, Phys. Lett. B **374**(1996)80.
- [21] M. Ciuchini, G. Degrassi, P. Gambino and G. F. Giudice, Nucl. Phys. B **527**(1998)21.
- [22] P. Ciafaloni, A. Romanino and A. Strumia, Nucl. Phys. B **524**(1998)361.
- [23] F.M. Borzumati, C. Greub, Phys. Rev. D **58**(1998)074004.
- [24] S. Bertolini, F. Borzumati, A. Masiero and G. Ridolfi, Nucl. Phys. B **353**(1991)591.
- [25] R. Barbieri and G. F. Giudice, Phys. Lett. B **309**(1993)86.
- [26] F. Borzumati and C. Greub, T. Hurth and D. Wyler, Phys. Rev. D **62**(2000)075005.
- [27] M. Causse and J. Orloff, Eur. Phys. J. C **23**(2002)749.
- [28] S. Prelovsek and D. Wyler, Phys. Lett. B **500**(2001)304.
- [29] M. Ciuchini, G. Degrassi, P. Gambino and G. F. Giudice, Nucl. Phys. B **534**(1998)3.
- [30] S. Bertolini and J. Matias, Phys. Rev. D **57**(1998)4197.
- [31] W. N. Cottingham, H. Mehrban and I. B. Whittingham, Phys. Rev. D **60**(1999)114029.
- [32] G. Barenboim and M. Raidal, Phys. Lett. B **457**(1999)109.
- [33] JoAnne L. Hewett, J. D. Wells, Phys. Rev. D **55**(1997)5549.
- [34] A. Ali, P. Ball, L. T. Handoko and G. Hiller, Phys. Rev. D **61**(2000)074024.
- [35] A. Masiero and L. Silvestrini, *Honolulu 1997, B physics and CP violation*, p.172 (hep-ph/9709244); *Erice 1997, Highlights of subnuclear physics* 404 (hep-ph/9711401).
- [36] M. Ciuchini *et al.*, JHEP **9810**(1998)008.
- [37] R. Contino, I. Scimemi, Eur. Phys. J. C **10**(1999)347.
- [38] F. Krauss, G. Soff, Nucl. Phys. B **633**(2002)237.
- [39] T.-F. Feng, X.-Q. Li, W.-G. Ma and F. Zhang, Phys. Rev. D **63**(2001)015013.
- [40] CMS Collaboration, Phys. Lett. B **716**(2012)30.
- [41] ATLAS Collaboration, Phys. Lett. B **716**(2012)1.
- [42] M. Aaboud *et.al*, ATLAS Collaboration, Phys. Rev. D **94**(2016)052009.
- [43] B. Adeva *et al.*, LHCb Collaboration, *Roadmap for selected key measurements of LHCb*,

arXiv:0912.4179.

- [44] T. Aushev *et al.*, *Physics at Super B Factory*, arXiv:1002.5012.
- [45] B. O’Leary *et al.*, SuperB Collaboration, *SuperB Progress Reports*, arXiv:1008.1541.
- [46] R. Barbier *et al.*, Phys. Rep. **420**(2005)1; C.-H. Chang, T.-F. Feng, Eur. Phys. J. C**12**(2000) 137.
- [47] P. Fileviez Perez and S. Spinner, Phys. Lett. B**673**(2009)251.
- [48] V. Barger, P. Fileviez Perez, and S. Spinner, Phys. Rev. Lett.**102**(2009)181802.
- [49] P. Fileviez Perez and S. Spinner, Phys. Rev. D**80**(2009)015004.
- [50] P. Fileviez Perez and S. Spinner, JHEP**1204**(2012)118.
- [51] V. Barger, P. Fileviez Perez and S. Spinner, Phys. Lett. B**696**(2011)509.
- [52] D. K. Ghosh, G. Senjanovic, Y. Zhang, Phys. Lett. B**698**(2011)420.
- [53] C.-H. Chang, T.-F. Feng, Y.-L. Yan, H.-B. Zhang, S.-M. Zhao, Phys. Rev. D**90**(2014)035013.
- [54] J. Hamann, S. Hannestad, G.G. Raffelt, I. Tamborra, and Y. Y. Y. Wong, Phys. Rev. Lett.**105**(2010)181301.
- [55] W. Altmannshofer, P. Ball, A. Bharucha, A. J. Buras, D. M. Straub, and M. Wick, JHEP0901(2009)019.
- [56] T.-F. Feng, Y.-L. Yan, H.-B. Zhang, and S.-M. Zhao, Phys. Rev. D**92**(2015)055024.
- [57] P. Gambino, M. Gorbahn and U. Haisch, Nucl. Phys. B**673**(2003)238.
- [58] G. Buchalla, A. J. Buras, M. E. Lautenbacher, Rev. Mod. Phys.**68**(1996)1125; N. Cabibbo, L. Manani, Phys. Lett. B**79**(1978)109; C. S. Kim, A. D. Martin, Phys. Lett. B**225**(1989)186.
- [59] T. Huber, T. Hurth, and E. Lunghi, Nucl. Phys. B**802**(2008)40.
- [60] K. A. Olive *et al.*(Particle Data Group), Chin. Phys. C,**38**(2014)090001.